

Debiasing Guidance for Discrete Diffusion with Sequential Monte Carlo

Lee Cheuk-Kit^{*1} Paul Jaha^{*2} Jes Frelsen² Pietro Lio¹ Michael Albergo^{3,4} Francisco Vargas¹

Abstract

Discrete diffusion models are a class of generative models that produce samples from an approximated data distribution within a discrete state space. Often, there is a need to target specific regions of the data distribution. Current guidance methods aim to sample from a distribution with mass proportional to $p_0(x_0)p(\zeta|x_0)^\alpha$ but fail to achieve this in practice. We introduce a Sequential Monte Carlo algorithm that generates unbiasedly from this target distribution, utilising the learnt unconditional and guided process. We validate our approach on low-dimensional distributions, controlled images and text generations. For text generation, our method provides strong control while maintaining low perplexity compared to guidance-based approaches.

1. Introduction

Discrete Diffusion models generate approximate samples from a data distribution $p_0(x_0)$ by gradually evolving samples from a simple base distribution $p_1(x_1)$ through a Continuous-Time Markov Chain (CTMC) (Shi et al., 2024; Campbell et al., 2022; Lou et al., 2024). While these models learn unconditional distributions, practical applications such as graph generation (Vignac et al., 2023), protein co-design (Campbell et al., 2024) or text generation (Lou et al., 2024) require controlled generation. For a conditioning variable ζ and temperature parameter α , we aim to sample from a tempered conditional distribution proportional to $p_0(x_0)p(\zeta|x_0)^\alpha$. When $\alpha = 1$, this recovers the conditional $p_0(x_0|\zeta)$. Higher values ($\alpha > 1$) biases sampling toward the conditioning signal ζ , while lower values ($\alpha < 1$) promotes diversity. To sample from this tempered distribution, guidance methods modify the unconditional diffusion transition rates (Nisonoff et al., 2024). However, guidance fails to

^{*}Equal contribution ¹University of Cambridge ²Technical University of Denmark ³Society of Fellows, Harvard University ⁴Institute for Artificial Intelligence and Fundamental Interactions, Massachusetts Institute of Technology. Correspondence to: Lee Cheuk-Kit <brianlee.lck@gmail.com>.

Preprint

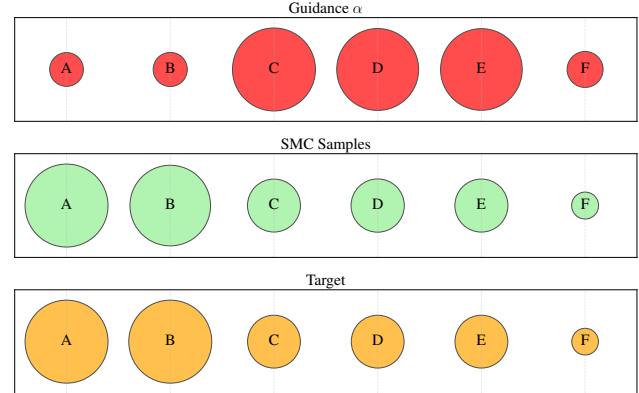


Figure 1. Visualization of a 1D discrete distribution with six states (A-F). The size of each disk represents probability mass. Orange circles show the target tempered distribution, green circles represent our SMC-based method which accurately approximates the target, while red circles show standard guidance failing to match the target distribution.

sample from the intended distribution (Chidambaram et al., 2024; Bradley & Nakkiran, 2024), producing corrupted samples at high α values (Chidambaram et al., 2024). Recent works propose finetuning approaches using reinforcement learning to sample from tempered distributions (Domingo-Enrich et al., 2025; Venkatraman et al., 2024; Fan et al., 2023; Black et al., 2024; Clark et al., 2024; Uehara et al., 2025). In this work, we address the theoretical and practical challenges of sampling from tempered distributions in discrete diffusion models. This work makes the following contributions:

1. We derive the exact transition rates required to sample from the tempered distribution with unnormalised mass $p_0(x_0)p(\zeta|x_0)^\alpha$ in discrete diffusion.
2. We propose an algorithm based on Sequential Monte Carlo, that asymptotically samples from the intended tempered distribution by exploiting previously forgone properties of the guided transition rate matrix, without any additional learning.
3. We validate our approach through low-dimensional experiments and demonstrate its effectiveness on controlled image and text generation, achieving strong conditional control with low perplexity on text dataset.

2. Background Work

2.1. Continuous Time Markov chains

A Continuous Time Markov Chain (CTMC) $\{X_t\}_{t \in [0,1]}$ is a Markov process on a finite state space $\mathcal{X} = \{1, \dots, S\}$. The evolution of X_t is governed by a time-dependent rate matrix $R_t : \mathcal{X} \times \mathcal{X} \rightarrow \mathbb{R}$, which defines infinitesimal transition probabilities $p_{t+\Delta t|t}(x_{t+\Delta t}|x_t)$ given by

$$\delta_{x_{t+\Delta t}, x_t} + R_t(x_t, x_{t+\Delta t})\Delta t + o(\Delta t), \quad (1)$$

where $\delta_{a,b}$ is 1 if $a = b$ and 0 otherwise.

The probability mass p_t of X_t evolves according to the Kolmogorov Forward Equation (KFE):

$$\partial_t p_t(x) = \underbrace{\sum_{y \neq x} p_t(y) R_t(y, x)}_{\text{incoming mass}} - \underbrace{\sum_{y \neq x} p_t(x) R_t(x, y)}_{\text{outgoing mass}}, \quad (2)$$

which can be written in vector form as:

$$\partial_t p_t = R_t^\top p_t, \quad (3)$$

where R_t satisfies mass conservation:

$$R_t(x, x) = - \sum_{y \neq x} R_t(x, y). \quad (4)$$

For simplicity, we define,

$$R_t(x) = \sum_{y \neq x} R_t(x, y) \quad (5)$$

To obtain approximate samples \tilde{X}_t , one may use the Euler sampling algorithm (Campbell et al., 2024), initialising $\tilde{X}_0 \sim p_0$ and updating subsequent samples in intervals of Δt following:

$$\tilde{X}_{t+\Delta t} \sim \tilde{p}_{t+\Delta t|t}^{\text{Euler}}(\cdot | \tilde{x}_t), \quad (6)$$

$$\tilde{p}_{t+\Delta t|t}^{\text{Euler}}(\tilde{x}_{t+\Delta t} | \tilde{x}_t) \propto \delta_{\tilde{x}_{t+\Delta t}, \tilde{x}_t} + R_t(\tilde{x}_t, \tilde{x}_{t+\Delta t})\Delta t. \quad (7)$$

A more comprehensive overview including the treatment of reverse-time CTMC can be found in Appendix B.

2.2. Discrete Diffusion Model

Discrete diffusion models are generative models that rely on a pair of stochastic processes: a forward process corrupting data distribution p_0 into base distribution p_1 , and its learned reverse process reconstructing p_0 from p_1 . Discrete diffusion models formulate these as Continuous Time Markov Chains on finite state spaces \mathcal{X} with $|\mathcal{X}| = S$. Discrete diffusion models require learning the reverse process. Campbell et al. (2022) learn the reverse rate matrix through likelihood objectives, while Lou et al. (2024) instead learn the reverse rate matrix using a score entropy objective. In their work,

they propose the masking diffusion model, which extends the state space \mathcal{X} with a masking state $\mathfrak{m} = S + 1$ to form an extended state space $\bar{\mathcal{X}} = \{1, \dots, S, \mathfrak{m}\}$. At time t , the masking process sends the current state to the masking state \mathfrak{m} according to a time-dependent noise schedule $\sigma : [0, 1] \rightarrow \mathbb{R}^+$, with transition probability $p_{t|0}^{\text{mask}}$:

$$p_{t|0}^{\text{mask}}(x_t|x_0) = \delta_{x_t, x_0} e^{-\sigma(t)} + \delta_{x_t, \mathfrak{m}} (1 - e^{-\sigma(t)}) \quad (8)$$

For sufficiently large $\sigma(1)$, the masking process mixes to a point mass at \mathfrak{m} at time $t = 1$. To sample from a masking diffusion model, we start at the masking state \mathfrak{m} at $t = 1$ and apply Euler sampling in reverse time with learned rate matrix \bar{R}_t . For high-dimensional data like text, the process extends to \mathcal{X}^d by corrupting each dimension independently (Shi et al., 2024).

3. Guidance

Let $\{X_t\}_{t \in [0,1]}$ be a reverse-time CTMC with probability mass p_t and rate matrix R_t . For a conditioning variable ζ , we write $p_t(\zeta|x_t)$ and $p_t(x_t|\zeta)$ as the conditioned probability density of ζ given $X_t = x_t$ and the conditioned probability mass of x_t given ζ respectively.

With guidance scale α , we aim to sample from the tempered distribution $p_0(x_0)p_0(\zeta|x_0)^\alpha/\mathcal{Z}_\alpha$, where \mathcal{Z}_α is a normalising constant. When $\alpha = 1$, this recovers $p_0(x_0|\zeta)$. Higher values ($\alpha > 1$) bias sampling toward high likelihood regions of ζ , while lower values promote diversity.

Guidance modifies R_t to R_t^α (Definition 3.1) under the premise that it samples correctly from the intended tempered distribution. However, guidance fails to do so when $\alpha \neq 1$ as shown in Figure 1.

Definition 3.1. The guided rate matrix R_t^α is defined as,

$$\forall x \neq y. R_t^\alpha(x, y|\zeta) = R_t(x, y) \left[\frac{p_t(\zeta|y)}{p_t(\zeta|x)} \right]^\alpha, \quad (9)$$

$$\forall x. R_t^\alpha(x, x|\zeta) = -R_t^\alpha(x|\zeta) \quad (10)$$

We defer the learning of guided rate matrix to Section 6.1. One might expect the guided rate matrix R_t^α to represent the time-reversal corrupting process starting at the tempered distribution $p_0(x_0)p_0(\zeta|x_0)^\alpha/\mathcal{Z}_\alpha$. However, as shown in Proposition 3.2, this is not the case.

Proposition 3.2. Let $M_t[\cdot]$ denote the evolution of probability mass at time t under the corrupting process $p_{t|0}^{\text{corrupt}}$ of X_t , the unconditional diffusion model. Define $p_t^{\alpha, \text{true}}$ as:

$$p_t^{\alpha, \text{true}} = M_t[p_0(\cdot) p_0(\zeta|\cdot)^\alpha / \mathcal{Z}_\alpha].$$

Then,

$$p_t^{\alpha, \text{true}}(x_t) \propto p_t(x_t) \mathbb{E}[p_0(\zeta | X_0)^\alpha | X_t = x_t].$$

The true tempered rate matrix $R_t^{\alpha, \text{true}}$ given by

$$\begin{aligned} \forall x \neq y, R_t^{\alpha, \text{true}}(x, y | \zeta) &= R_t(x, y) \frac{\mathbb{E}[p_0(\zeta | X_0)^\alpha | X_t = y]}{\mathbb{E}[p_0(\zeta | X_0)^\alpha | X_t = x]}, \\ \forall x, R_t^{\alpha, \text{true}}(x, x | \zeta) &= - \sum_{y \neq x} R_t^{\alpha, \text{true}}(x, y | \zeta), \end{aligned}$$

is rate matrix of time reversal of the corruption process starting from $p_0(\cdot) p_0(\zeta | \cdot)^\alpha / \mathcal{Z}_\alpha$

From Proposition 3.2, it follows that $R_t^\alpha = R_t^{\alpha, \text{true}}$ holds only for $\alpha = 1$. Furthermore, for $\alpha = 1$, guidance requires that the base distribution p_1 is independent of the conditioning variable ζ to correctly sample from the conditioned distribution $p_0(X_0 | \zeta)$, as shown in Corollary 3.3.

Corollary 3.3. *If $p_1(x_1 | \zeta) = p_1(x_1)$, then guidance samples correctly from the conditioned distribution $p_0(x_0 | \zeta)$.*

While (Nisonoff et al., 2024) presents similar results to Corollary 3.3, our lemma establishes that the independence condition is necessary.

Learning $R_t^{\alpha, \text{true}}$ most often requires expensive simulation-based objectives to estimate the gradients of a reverse pathwise KL divergence (Domingo-Enrich et al., 2025; Denker et al., 2024; Uehara et al., 2025). Therefore, we focus instead on sampling from $p_t^\alpha(x_t) \propto p_t(x) p_t(\zeta | x_t)^\alpha$.

4. Debiasing Guidance with Sequential Monte Carlo

Our objective is to sample from the tempered distribution $\frac{1}{\mathcal{Z}_0^\alpha} p_0(x_0) p_0(\zeta | x_0)^\alpha$. To that end, we first introduce an importance sampling method, which we later leverage through resampling.

4.1. Importance Sampling the Tempered Distribution

We consider the importance sampling method to compute the expectation of a function h under the distribution of probability mass $p_t^\alpha(x_t) = \frac{1}{\mathcal{Z}_t^\alpha} p_t(x_t) p_t(\zeta | x_t)^\alpha$ where \mathcal{Z}_t^α is the normalising constant. We write the expectation as:

$$\mathbb{E}_{x \sim p_t^\alpha} [h(x)] = \frac{1}{\mathcal{Z}_t^\alpha} \sum_{x \in \mathcal{X}} h(x) p_t(x) p_t(\zeta | x_t)^\alpha, \quad (11)$$

For importance sampling, we consider a proposal in the form of a reverse time CTMC $\{Y_t\}_{t \in [0,1]}$, with rate matrix Q_t and initial distribution p_1 . We construct unnormalised importance weight $\{W_t\}_{t \in [0,1]}$ such that:

$$\mathbb{E}_{x \sim p_t^\alpha} [h(x)] = \frac{\mathbb{E}[W_t \cdot h(Y_t)]}{\mathbb{E}[W_t]} \quad (12)$$

where \mathbb{E} is an expectation over the joint distribution $\text{Law}(W_t, Y_t)$.

Proposition 4.1 provides one form of the unnormalised importance weights $\{W_t\}_{t \in [0,1]}$.

Proposition 4.1. *Let proposal $\{Y_t\}_{t \in [0,1]}$ be a reverse-time CTMC with rate matrix Q_t and initial distribution $p_1(\cdot)$. Define $\{W_t\}_{t \in [0,1]}$ by*

$$W_t = \frac{d\mathbb{P}_t^{\text{base}}}{dQ_t} \left(\frac{d\mathbb{P}_t^{\alpha=1}}{d\mathbb{P}_t^{\text{base}}} \right)^\alpha,$$

where we have path space measures $\mathbb{P}_t^{\text{base}} = \text{Law}\{X_\tau\}_{\tau \in [t,1]}$, $\mathbb{P}_t^{\alpha=1} = \text{Law}\{X_\tau | \zeta\}_{\tau \in [t,1]}$ and $Q_t = \text{Law}\{Y_\tau\}_{\tau \in [t,1]}$.

Then the Radon-Nikodym derivatives can be written as,

$$\begin{aligned} \ln \frac{d\mathbb{P}_t^{\text{base}}}{dQ_t} &= \sum_{\substack{\tau \geq t \\ Y_{\tau+} \neq Y_\tau}} \ln R_t(Y_{\tau+}, Y_\tau) \\ &\quad + \int_1^t Q_\tau(Y_t) - R_\tau(Y_t) d\tau \end{aligned}$$

and

$$\begin{aligned} \ln \frac{d\mathbb{P}_t^{\alpha=1}}{d\mathbb{P}_t^{\text{base}}} &= \sum_{\substack{\tau \geq t \\ Y_{\tau+} \neq Y_\tau}} \ln R_t^{\alpha=1}(Y_{\tau+}, Y_\tau | \zeta) \\ &\quad + \int_1^t R_\tau(Y_\tau) - R_\tau^{\alpha=1}(Y_\tau | \zeta) d\tau, \end{aligned}$$

such that for any p_t^α -integrable function h and time $t \in [0, 1]$, we have

$$\mathbb{E}_{x \sim p_t^\alpha} [h(x)] = \frac{\mathbb{E}[W_t \cdot h(Y_t)]}{\mathbb{E}[W_t]},$$

where the expectation is taken over $\text{Law}(W_t, Y_t)$

A proof of the proposition can be found in Appendix D. Due to the modular nature of our result, it seamlessly extends to stochastic differential equations for more details please see Appendix D.1.

For practical implementation, we approximate the CTMC by discretising time into T steps: $1 = t_1 > t_2 > \dots > t_T = 0$. For times $t < s$, we denote the transitions derived from rate matrices Q_t , R_t , and $R_t^{\alpha=1}$ as $q_{t|s}(x_t | x_s)$, $p_{t|s}(x_t | x_s)$, and $p_{t|s}(x_t | x_s, \zeta)$ respectively. To this end, we consider a discretisation of Proposition 4.1 in Appendix E. We also present Algorithm 1 in Section 4.2, a pseudo-code of the discretised version of the proposed sampling method.

4.2. Resampling and Sequential Monte Carlo

To approximate sample from the tempered distribution p_0^α , we leverage resampling. Given a set of K weights and samples $(w_t^{(i)}, y_t^{(i)}) \sim \text{Law}(W_t, Y_t)$, resampling allows us to obtain approximate samples from p_t^α by sampling the Categorical distribution,

$$\text{Cat} \left(\left\{ \frac{w_t^{(i)}}{\sum_{j=1}^K w_t^{(j)}} \right\}_{i=1}^K, y_t^{(i)} \right), \quad (13)$$

where $y_t^{(i)}$ is sampled with probability $\frac{w_t^{(i)}}{\sum_{j=1}^K w_t^{(j)}}$.

This suggests an algorithm to obtain samples from the tempered distribution $p_0(x_0)p_0(\zeta|x_0)^\alpha$ by resampling at time $t = 0$. However, this approach suffers from a significant challenge: weight degeneracy. As t approaches 0, the variance of weights W_t increases dramatically, requiring an impractical number of samples.

Sequential Monte Carlo (SMC) addresses this challenge by performing resampling steps at intermediate times $0 < t < 1$, obtaining approximate samples of p_t^α while resetting the weights to maintain the importance sampling equality. Effectively, this eliminates sample from low likelihood regions and duplicates those in high likelihood regions.

The resampling step is flexible in both algorithm choice and timing. In Section 6.3, we explore partial resampling where only a subset of samples participate. Resampling is typically triggered when the effective sample size (ESS) falls below a threshold, where ESS is defined as:

$$\text{ESS}_t^K = \left(\sum_{i=1}^K w_t^{(i)} \right)^2 / \sum_{i=1}^K (w_t^{(i)})^2 \in [1, K] \quad (14)$$

We emphasize that the resampling procedure allows us to leverage importance sampling to generate asymptotically unbiased samples rather than purely computing expectations. The full algorithm to sample from the tempered distribution can be found in Algorithm 1 detailed in Algo. 2 (App. F) for our experiments.

5. Numerical Verification

We validate our algorithm’s ability to sample from the tempered distribution $p_0(x_0)p_0(\zeta|x_0)^\alpha / \mathcal{Z}_\alpha$ using low-dimensional examples. These experiments use explicitly specified probability mass $p_0(x_0)$ and conditional likelihood $p_0(\zeta|x_0)$, enabling direct computation of the guided ratio matrix. This setup verifies algorithmic correctness independent of learning effects and allows evaluation of the KL divergence between sampled and target distributions.

Experimental setup We evaluate on state spaces of dimension one (\mathcal{V}) and two (\mathcal{V}^2), where \mathcal{V} is a finite vocab-

Algorithm 1 Main Algorithm

Require: Number of particles K ; Proposal Rate Matrix Q_t ; Unconditional rate matrix R_t ; Time grid $\{t_l\}_{l=1}^T$ for potential resampling; ESS threshold ESS.THRESHOLD; Resampling algorithm `resample`.

- 1: **Initialisation:**
- 2: Sample $\{y_1^{(i)}\}_{i=1}^K$ i.i.d. from p_1 .
- 3: Set $\hat{w}_1^{(i)} \leftarrow 1$ for $i = 1, \dots, K$.
- 4: **for** $l = 1$ to T **do**
- 5: **for** $i = 1$ to K **do**
- 6: {Step 1: Evolve samples and weights}
- 7: Obtain $(y_{l+1}^{(i)}, \hat{w}_{l+1}^{(i)})$ by evolving joint system (Y_t, W_t) from $(y_l^{(i)}, \hat{w}_l^{(i)})$ at time t_l
- 8: **end for**
- 9: {Step 3: Resample; see Appendix G for other resampling algorithms}
- 10: Set $\text{ESS} \leftarrow \left(\sum_{i=1}^K \hat{w}_l^{(i)} \right)^2 / \sum_{i=1}^K (\hat{w}_l^{(i)})^2$
- 11: **if** $\text{ESS} \leq \text{ESS_THRESHOLD}$ **then**
- 12: Set $y_{l+1}^{(i)}, \hat{w}_{l+1}^{(i)} \leftarrow \text{resample}(\{y_l^{(i)}\}, \{\hat{w}_l^{(i)}\})$
- 13: **end if**
- 14: **end for**
- 15: **Output:**
- 16: Particles $\{x_T^{(i)}\}_{i=1}^K$

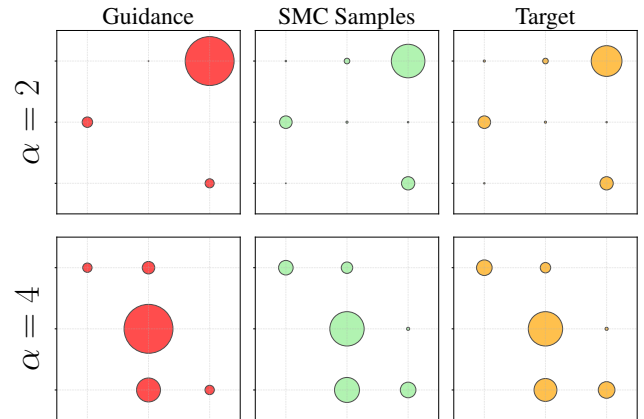


Figure 2. A two dimensional discrete distribution with nine states. The target distribution is in orange, standard guidance is in red and our SMC based method in green Top panel shows $\alpha = 2$, bottom panel $\alpha = 4$. In both cases, guidance-based sampling deviates from the target distribution, while SMC samples are significantly closer.

ulary. Our proposal uses per-dimension Euler sampling (Campbell et al., 2024) with 100 discretization steps and 50,000 samples. For each dimension, we generate 30 different tempered target distributions $\pi \propto p_0(x_0)p_0(\zeta|x_0)^\alpha$ by combining different choices of $p_0(x_0)$, $p_0(\zeta|x_0)$, and

temperature α . We sample from each target using both guidance and SMC, then compute KL divergences between the true tempered distribution and the empirical distributions σ^{SMC} and σ^{Guided} . Results in Table 1 show that guided processes significantly deviate from targets while SMC achieves approximate sampling, demonstrating superior sampling across all combinations. Qualitative examples are shown in Figures 1 and 2.

Dimension	$ \mathcal{V} $	$\text{KL}(\pi \sigma^{\text{SMC}})$	$\text{KL}(\pi \sigma^{\text{Guided}})$
1	50	0.002 \pm 0.001	0.004 \pm 0.003
2	3	0.035 \pm 0.179	0.074 \pm 0.082
2	10	0.013 \pm 0.012	0.081 \pm 0.052
2	100	1.725 \pm 0.743	6.690 \pm 1.194
2	200	5.948 \pm 1.042	12.906 \pm 0.542

Table 1. Forward KL divergence between the target tempered distribution π and the empirical distribution of samples from the guided process and SMC algorithm. Method with a lower KL divergence is highlighted.

6. Experiments

Section 5 demonstrated SMC’s ability to sample tempered distributions with sufficient particles and discretisation steps. In practice, for image and text generation tasks, computing rate matrices is computationally intensive, limiting feasible particle counts and step sizes. For these practical settings, we use the guided rate matrix as our proposal in SMC, with guidance temperature β distinct from the SMC temperature α , and provide guidance on resampling strategies.

6.1. Learning the Guidance Term

We consider two approaches to obtain the guided rate matrix R_t^α , **DEFT** and **CFG**.

DEFT For discrete diffusion models, we extend Doob’s h-transform Efficient FineTuning (DEFT, Denker et al. (2024)) by showing that the conditional rate matrix $R_t^{\alpha=1}$ decomposes into an unconditional rate matrix R_t and a guidance term $p_t(\zeta|y)/p_t(\zeta|x)$: $R_t^{\alpha=1}(x, y) = R_t(x, y) \times p_t(\zeta|y)/p_t(\zeta|x)$. We model the guidance term with a neural network g and parameterize the conditional rate matrix as $R_t^{\alpha=1}(x, y|\zeta) = R_t(x, y)g(x, y, t)$ while keeping the unconditional rate parameters fixed. We use this guidance term in both pixel level image generation and controlled text generation.

CFG In text generation, we extend classifier-free guidance (Ho & Salimans, 2022a). We obtain the conditional rate matrix $R_t^{\alpha=1}(x, y|\zeta)$ by finetuning the learned unconditional rate matrix $R_t(x, y|\zeta)$, concatenating conditions to the inputs. For $\alpha > 1$, the guided rate matrix follows

$$[p_t(\zeta|y)/p_t(\zeta|x)]^\alpha = [R_t^{\alpha=1}(x, y|\zeta)/R_t(x, y)]^\alpha$$

There are other ways of finding a guided rate matrix. Nisonoff et al. (2024); Vignac et al. (2023) consider a first-order Taylor approximation of the guidance term; Kerby & Moon (2024); Li et al. (2024) consider a training-free approach by Monte Carlo estimates of the guidance term.

In what follows we present results where we adopted the CFG approach and refer the reader to Appendix H for results with DEFT. We first discuss partial resampling, a key component of our SMC implementation, and then detail our experiments and findings.

6.2. Partial Resampling

SMC methods suffer from mode collapse in high dimensions when using few particles. In this scenario, most particle weights decay rapidly, leaving only a small subset with significant weights. During resampling, particles with low weights are discarded, often resulting in only one or two unique particles. Figure 3 (middle) demonstrates this effect: a batch of 16 particles collapses into identical images.

We adopt a partial resampling scheme which effectively mitigates mode collapse by resampling only a subset of particles. We select the K most and least weighted samples for resampling, which preserves sample diversity and maintains unbiased sampling from the target distribution as shown in Figure 3 (right). We detail partial resampling algorithms in Appendix G. In our experiments, we use Algorithm 4, set $K = \lfloor N/4 \rfloor$, resampling half of all generated samples.

6.3. Class-Conditional Pixel-Level Image Generation

We evaluate our method on MNIST class-conditional generation using 28×28 grayscale images with pixel values in $\{0, \dots, 255\}$. We first detail the experimental setup; we then study partial resampling for mitigating mode collapse in SMC and analyze its impact on generation control.

6.3.1. DATASET AND TRAINING DETAILS

We train an unconditional SEDD model (Lou et al., 2024) parameterized by a U-Net (Ronneberger et al., 2015) for 20k steps. Using 20% of MNIST, we finetune a guidance network for 4k steps with DEFT using the SEDD denoising score entropy loss. The guidance network is a U-Net with learned condition embeddings added to each layer, at 50% parameters of the unconditional network.

6.3.2. DOES PARTIAL RESAMPLING MITIGATE MODE COLLAPSE?

The MNIST dataset visually demonstrates mode collapse and the effectiveness of partial resampling (Section 6.2). Using SMC with guidance temperature $\beta = 1$ and SMC

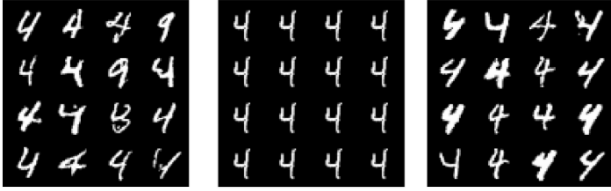


Figure 3. **Class-Conditioned Image Generation** $\zeta = 4$: From left to right: Independent guidance samples, SMC samples without partial resampling, and SMC samples with partial resampling. SMC with partial resampling generates high-quality samples of digit 4 while avoiding mode collapse.

temperature $\alpha = 3$, we observe mode collapse in Figure 3 (center), where 16 particles converge to identical images. Partial resampling (Figure 3, right) maintains both diversity and stronger conditional control compared to naive guidance (Figure 3, left), which occasionally generates incorrect digits.

6.3.3. DOES SMC IMPROVE CONDITIONAL CONTROL?

For class-conditioned generation, we evaluate sample consistency with target conditions using a pre-trained digit classifier. Figure 4 shows accuracy for SMC temperatures $\alpha \in \{1, 2, 3\}$ and N number of particle in $\{5, 10, 20, 50, 100\}$, using $R_t^{\alpha=1}$ as the proposal. We compute accuracies within each SMC run and confidence intervals across 10 independent runs. Higher SMC temperatures yield better accuracy across all particle counts. Partial resampling achieves higher accuracy with lower variance, which indicates that it effectively reduces mode collapse.

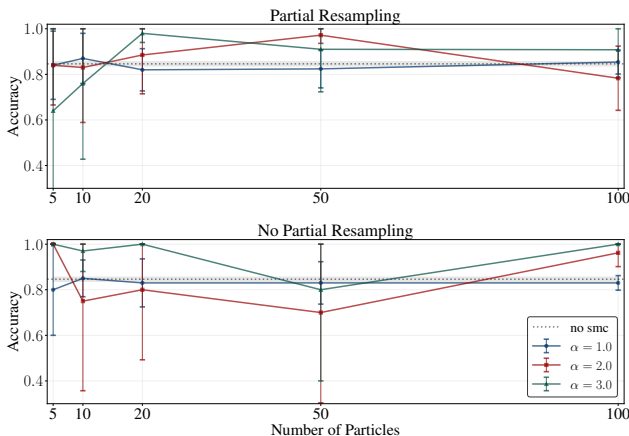


Figure 4. **Accuracy on Class-Conditioned Image generation.** SMC classification accuracy versus particle count for different twist temperatures (α), with and without partial resampling. Partial resampling and higher α achieve better peak accuracy. Dotted lines show baseline accuracy without SMC. Values averaged over 50 runs.

Experiments on MNIST demonstrate that our method successfully addresses two key challenges in conditional generation. Partial resampling effectively mitigates mode collapse while maintaining sample diversity, and higher SMC temperatures improve conditional control across all particle counts. These results validate our theoretical framework on a standard image generation task.

6.4. Controlled Text Generation

We validate the approach on three controlled text generation: Sentiment Controlled Generation, Toxicity Controlled Generation, and Text Infilling. These high-dimensional experiments demonstrates the algorithm practicality.

6.4.1. DATASET AND TRAINING DETAILS

In all experiments, we use the pre-trained 320M non-embedding parameters `sedd-medium`, a Score Entropy Discrete Diffusion (SEDD) model (Lou et al., 2024). When guiding with CFG we finetune `sedd-medium` and when guiding with DEFT we finetune `sedd-small` for 2k steps to serve as the guidance term $p_t(\zeta|y)/p_t(\zeta|x)$ for the large `sedd-medium` model, on task-specific datasets:

Toxicity Controlled Generation Following (Liu et al., 2021), we use human-annotated comments from the Jigsaw Unintended Bias in Toxicity Classification challenge¹, with texts labeled toxic when 50% or more annotators mark them as such. A prompt `The generated text is toxic` is concatenated to the transformer input as the condition.

Sentiment Controlled Generation. We follow the setup in (Amini et al., 2024), using the Stanford Sentiment Treebank, a dataset of movie reviews, as the finetuning dataset. A prompt `The generated text is of positive sentiment` or `The generated text is of negative sentiment` is concatenated to the transformer input as the condition.

Text Infilling. We finetune on 10% of the OpenWebText training dataset. For each sentence, randomly sampled indices (START, END) define the token range to mask. The masked sentence ζ is concatenated to the model input throughout generation. The entire partial masked sentence [PREFIX] [MASK] [SUFFIX] is passed to the network as the condition.

We evaluate samples using both fluency and conditional control metrics, averaging across 5 runs and 50 particles for SMC or 250 particles for guidance, with 100 discretisation steps and we employ partial resampling. For fluency, we compute generative perplexity (Liu et al., 2021) using GPT2-XL as the reference model, which quantifies

¹<https://bit.ly/3cvG5py>

how likely a sentence is to appear in the reference model. For sentiment and toxicity tasks, we use a LoRA-finetuned GPT2-XL to account for stylistic differences in the finetuning dataset. For conditional metrics, we use a pre-trained classifier for sentiment accuracy, Perspective API for toxicity scores, and measure how many unmasked tokens are successfully generated.

6.4.2. ABLATING GUIDANCE AND SMC TEMPERATURE

We study how guidance temperature β and SMC temperature α impact both conditional control and fluency metrics across toxicity, sentiment, and infilling tasks.

Our findings SMC-based methods improve considerably on conditional control metrics for low-to-mid guidance temperature β and with high SMC temperature α . For high guidance temperature, the guidance baseline improves conditional metrics but at the cost of higher perplexity. This implies that guidance-generated samples drift from the distribution of the fine-tuning dataset. Hence, we conclude that the optimal approach is to combine SMC with high SMC temperature and mid-to-low guidance temperature.

In more detail, Figure 5, Figure 6, and Figure 7 show the generative perplexity and performance metrics across guidance temperature $\beta = \{0.0, 0.2, 0.4, 0.6, 0.8, 1.0, 1.2, 1.4, 1.6, 1.8, 2.0\}$ and SMC temperature $\alpha = \{1, 2, 4, 8\}$. Across all three tasks, SMC methods with high SMC temperature α consistently outperform the guidance method. For high guidance temperature β the gap between SMC and the guidance method reduces. However, perplexity deteriorates at high guidance temperature which indicates that the proposal is unable to sample from high likelihood region of the target tempered distribution.

For toxicity control, SMC consistently achieves better toxicity scores until $\beta > 1.4$, while maintaining comparable perplexity. In sentiment control, SMC shows improved accuracy until $\beta > 1.2$, with slightly higher perplexity. At $\beta > 1.4$ and $\alpha = 1$, SMC achieves lower perplexity than standard guidance while maintaining the same accuracy as the other methods. For text infilling, SMC shows superior or on-par accuracy across all guidance temperatures and better perplexity for $\beta \in \{0.4, 0.6\}$; or at $\alpha = 1$ and $\beta > 1.4$ SMC shows reduced perplexity while maintaining the same accuracy. As β increases beyond 1.4, we observe a common pattern across all tasks: the performance gap between SMC and guidance narrows, but at the cost of significant perplexity deterioration, particularly for higher β values.

6.4.3. SCALING UP DISCRETISATION STEP

We further investigate sample qualities by increasing discretization steps to 1000, effectively allocating 10x compute. For text infilling, we employ two additional metrics:

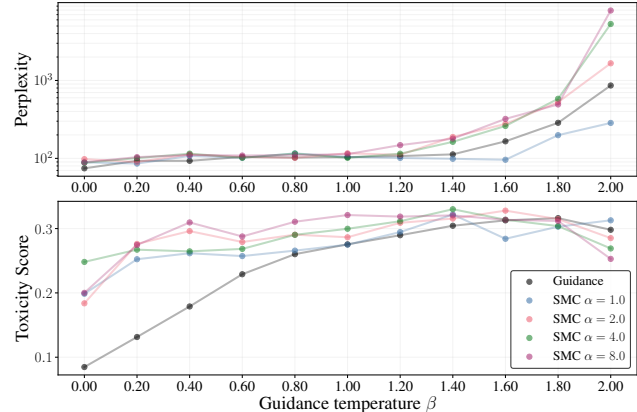


Figure 5. **Toxicity controlled generation:** SMC methods show improved toxicity scores across all guidance temperatures β , demonstrating enhanced generation control. While baseline performance matches SMC at high β values, the perplexity deteriorates significantly.

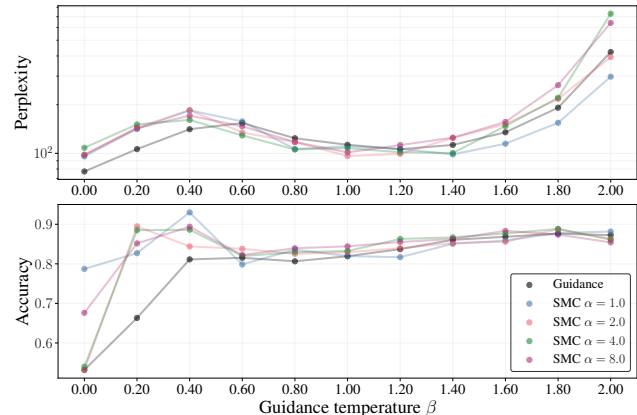


Figure 6. **Sentiment control generation:** For guidance temperatures $\beta \in \{0.2, 0.4\}$, SMC approaches achieve notably better accuracy compared to guidance, though at the cost of slightly higher perplexity. For guidance temperature greater than 1.4 and for $\alpha = 1$, SMC method achieves lower perplexity compared to guidance.

BERTScore (Zhang* et al., 2020) with the DeBERTa model (He et al., 2021), and GLEU-4 (Wu et al., 2016). For sentiment and toxicity controlled generation, we compare against a baseline prompting method, while for infilling, we evaluate against a reconstruction method that overwrites the sampling trajectory with the partially masked sentence.

Table 4, Table 2, and Table 3 summarise our empirical results. SMC with a high SMC temperature significantly outperforms the base guidance method across all tasks. Notably, for toxicity and sentiment-controlled generation, our SMC-based method significantly outperforms a simple prompting strategy in generating strong conditions. However, for in-

Debiasing Guidance for Discrete Diffusion with Sequential Monte Carlo

Method	Sequential Monte Carlo								Guidance		Prompting
	1.0		2.0		4.0		8.0		N/A		N/A
SMC Temp. α	1.0		2.0		4.0		8.0		N/A		N/A
Guidance Temp. β	1.0	1.2	1.0	1.2	1.0	1.2	1.0	1.2	1.0	1.2	N/A
Perplexity	84.410±8.647	93.225±7.281	80.500±3.554	83.767±7.457	77.538±11.209	85.170±7.253	80.283±6.825	78.388±6.606	80.283±6.825	78.388±6.606	44.673±11.687
Accuracy \uparrow	0.839±0.047	0.840±0.065	0.882±0.048	0.877±0.050	0.875±0.048	0.872±0.057	0.868±0.059	0.875±0.060	0.837±0.006	0.837±0.006	0.548±0.105

Table 2. Performance metrics for **sentiment control** using Sequential Monte Carlo, Guidance, and Prompting. Light blue marks the best performing method.

Method	Sequential Monte Carlo								Guidance		Prompting
	1.0		2.0		4.0		8.0		N/A		N/A
SMC Temp. α	1.0		2.0		4.0		8.0		N/A		N/A
Guidance Temp. β	1.0	1.2	1.0	1.2	1.0	1.2	1.0	1.2	1.0	1.2	N/A
Perplexity	66.558±9.085	58.913±1.945	62.192±6.998	88.650±3.325	89.125±4.062	109.200±3.518	77.000±13.420	88.800±1.549	67.475±8.467	70.525±10.079	44.319±13.885
Toxicity \uparrow	0.451±0.244	0.384±0.231	0.577±0.232	0.547±0.222	0.595±0.231	0.611±0.208	0.561±0.252	0.558±0.230	0.455±0.244	0.505±0.246	0.130±0.123

Table 3. Performance metrics for **toxicity control** using Sequential Monte Carlo, Guidance, and Prompting. Light blue marks the best performing method.

Method	Sequential Monte Carlo				Guidance	Reconstruction
	1.0	2.0	4.0	8.0	N/A	N/A
SMC Temp. α	1.0	2.0	4.0	8.0	N/A	N/A
Guidance Temp. β	1.0	1.0	1.0	1.0	1.0	N/A
Perplexity	65.048±30.951	67.062±42.959	73.562±26.980	80.583±45.478	63.915±31.375	53.697±26.543
BERTScore \uparrow	0.583±0.038	0.584±0.032	0.587±0.029	0.576±0.038	0.583±0.037	0.595±0.038
GLEU \uparrow	0.701±0.021	0.703±0.022	0.708±0.019	0.699±0.022	0.701±0.021	0.706±0.021
Accuracy \uparrow	0.992±0.015	0.996±0.014	0.998±0.013	0.998±0.015	0.991±0.018	1.000±0.000

Table 4. Performance of guidance methods on text infilling: Sequential Monte Carlo (varying twist temperature α) plus a row of guidance temperature (all set to 1.0), Guidance, and Reconstruction guidance. Values show mean \pm standard deviation. \uparrow/\downarrow indicate better performance for higher/lower values. Light blue cell marks the best result. Light green cell marks the best result between Guidance and SMC.

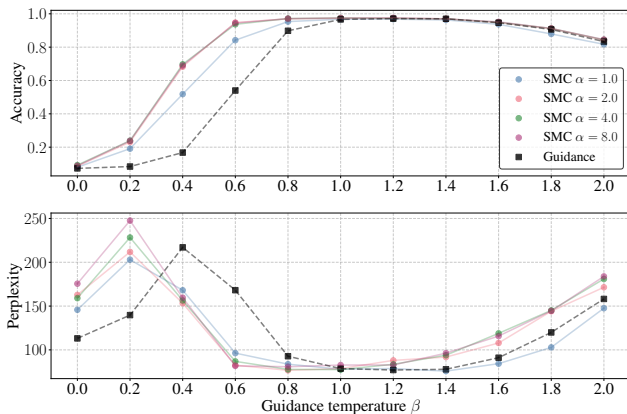


Figure 7. **Text infilling**: SMC method shows improved accuracy scores across guidance temperature. In addition for $\beta \in \{0.4, 0.6\}$ SMC methods show in addition improved perplexity, as well as for $\beta \geq 1.6$ and $\alpha = 1$.

filing and despite their theoretical guarantees, guidance and SMC approaches underperform compared to the reconstruction method, even though it is known to be biased (Wu et al., 2024). This indicates an inadequate learning

of the guided rate matrix. While SMC can strengthen the base guidance method, it cannot fully compensate for an imperfectly learned guided rate matrix.

7. Conclusion and Future Work

This work addresses a fundamental challenge in diffusion models: accurate sampling from tempered distribution. We make three key contributions. First, we derive the exact transition rate to sample from the tempered distribution; second, we propose an SMC-based algorithm that asymptotically samples from the tempered distribution; third, we demonstrate its practicality in controlled generation. Our empirical results validate the practicality of our theoretically correct algorithm. In low dimensions, it significantly outperforms standard guidance methods. In high dimensions, our method achieves superior control while maintaining sample quality. However, our experiments also reveal that the effectiveness depends on the quality of the learned guided rate matrix. Lastly, Proposition 4.1 transfers naturally to continuous diffusion models, which represents a promising avenue for future research.

Acknowledgement

The authors would like to thank Junhua Chen for extensive discussions on the implementation of Sequential Monte Carlo Methods.

Impact Statement

This paper presents work whose goal is to advance the field of Machine Learning. There are many potential societal consequences of our work, none which we feel must be specifically highlighted here.

References

- Albergo, M. S. and Vanden-Eijnden, E. Building normalizing flows with stochastic interpolants, 2023. URL <https://arxiv.org/abs/2209.15571>.
- Albergo, M. S. and Vanden-Eijnden, E. Nets: A non-equilibrium transport sampler. *arXiv preprint arXiv:2410.02711*, 2024.
- Albergo, M. S., Boffi, N. M., and Vanden-Eijnden, E. Stochastic interpolants: A unifying framework for flows and diffusions, 2023. URL <https://arxiv.org/abs/2303.08797>.
- Amini, A., Du, L., and Cotterell, R. Structured voronoi sampling, 2024. URL <https://arxiv.org/abs/2306.03061>.
- Black, K., Janner, M., Du, Y., Kostrikov, I., and Levine, S. Training diffusion models with reinforcement learning, 2024. URL <https://arxiv.org/abs/2305.13301>.
- Blattmann, A., Dockhorn, T., Kulal, S., Mendelevitch, D., Kilian, M., Lorenz, D., Levi, Y., English, Z., Voleti, V., Letts, A., Jampani, V., and Rombach, R. Stable video diffusion: Scaling latent video diffusion models to large datasets, 2023. URL <https://arxiv.org/abs/2311.15127>.
- Bradley, A. and Nakkiran, P. Classifier-free guidance is a predictor-corrector, 2024. URL <https://arxiv.org/abs/2408.09000>.
- Campbell, A., Benton, J., Bortoli, V. D., Rainforth, T., Deligiannidis, G., and Doucet, A. A continuous time framework for discrete denoising models, 2022. URL <https://arxiv.org/abs/2205.14987>.
- Campbell, A., Yim, J., Barzilay, R., Rainforth, T., and Jaakkola, T. S. Generative flows on discrete state-spaces: Enabling multimodal flows with applications to protein co-design. In *Forty-first International Conference on Machine Learning, ICML 2024, Vienna, Austria, July 21-27, 2024*. OpenReview.net, 2024. URL <https://openreview.net/forum?id=kQwSbv0BR4>.
- Carbone, D., Hua, M., Coste, S., and Vanden-Eijnden, E. Efficient training of energy-based models using jarzynski equality. *Advances in Neural Information Processing Systems*, 36:52583–52614, 2023.
- Chidambaram, M., Gatmiry, K., Chen, S., Lee, H., and Lu, J. What does guidance do? a fine-grained analysis in a simple setting, 2024. URL <https://arxiv.org/abs/2409.13074>.
- Clark, K., Vicol, P., Swersky, K., and Fleet, D. J. Directly fine-tuning diffusion models on differentiable rewards, 2024. URL <https://arxiv.org/abs/2309.17400>.
- Cornet, F. R. J., Bartosh, G., Schmidt, M. N., and Naesseth, C. A. Equivariant neural diffusion for molecule generation. In *The Thirty-eighth Annual Conference on Neural Information Processing Systems*, 2024. URL <https://openreview.net/forum?id=40pE5pFhWl>.
- Del Moral, P. and Penev, S. *Stochastic processes: From applications to theory*. CRC Press, Taylor & Francis Group, 2017.
- Denker, A., Vargas, F., Padhy, S., Didi, K., Mathis, S. V., Dutordoir, V., Barbano, R., Mathieu, E., Komorowska, U. J., and Lio, P. DEFT: efficient finetuning of conditional diffusion models by learning the generalised h-transform. *CoRR*, abs/2406.01781, 2024. doi: 10.48550/ARXIV.2406.01781. URL <https://doi.org/10.48550/arXiv.2406.01781>.
- Dhariwal, P. and Nichol, A. Diffusion models beat gans on image synthesis, 2021. URL <https://arxiv.org/abs/2105.05233>.
- Domingo-Enrich, C., Drozdal, M., Karrer, B., and Chen, R. T. Q. Adjoint matching: Fine-tuning flow and diffusion generative models with memoryless stochastic optimal control, 2025. URL <https://arxiv.org/abs/2409.08861>.
- Fan, Y., Watkins, O., Du, Y., Liu, H., Ryu, M., Boutilier, C., Abbeel, P., Ghavamzadeh, M., Lee, K., and Lee, K. Dpok: Reinforcement learning for fine-tuning text-to-image diffusion models. In Oh, A., Naumann, T., Globerson, A., Saenko, K., Hardt, M., and Levine, S. (eds.), *Advances in Neural Information Processing Systems*, volume 36, pp. 79858–79885. Curran Associates, Inc., 2023.
- Gulrajani, I. and Hashimoto, T. B. Likelihood-based diffusion language models, 2023. URL <https://arxiv.org/abs/2305.18619>.

- He, P., Liu, X., Gao, J., and Chen, W. Deberta: Decoding-enhanced bert with disentangled attention, 2021. URL <https://arxiv.org/abs/2006.03654>.
- Ho, J. and Salimans, T. Classifier-free diffusion guidance, 2022a. URL <https://arxiv.org/abs/2207.12598>.
- Ho, J. and Salimans, T. Classifier-free diffusion guidance, 2022b. URL <https://arxiv.org/abs/2207.12598>.
- Ho, J., Jain, A., and Abbeel, P. Denoising diffusion probabilistic models, 2020. URL <https://arxiv.org/abs/2006.11239>.
- Hoogeboom, E., Satorras, V. G., Vignac, C., and Welling, M. Equivariant diffusion for molecule generation in 3d, 2022. URL <https://arxiv.org/abs/2203.17003>.
- Kerby, T. J. and Moon, K. R. Training-free guidance for discrete diffusion models for molecular generation, 2024. URL <https://arxiv.org/abs/2409.07359>.
- Langley, P. Crafting papers on machine learning. In Langley, P. (ed.), *Proceedings of the 17th International Conference on Machine Learning (ICML 2000)*, pp. 1207–1216, Stanford, CA, 2000. Morgan Kaufmann.
- Léonard, C. Some properties of path measures. *Séminaire de Probabilités XLVI*, pp. 207–230, 2014.
- Li, X., Zhao, Y., Wang, C., Scalia, G., Eraslan, G., Nair, S., Biancalani, T., Ji, S., Regev, A., Levine, S., and Uehara, M. Derivative-free guidance in continuous and discrete diffusion models with soft value-based decoding, 2024. URL <https://arxiv.org/abs/2408.08252>.
- Lipman, Y., Chen, R. T. Q., Ben-Hamu, H., Nickel, M., and Le, M. Flow matching for generative modeling, 2023. URL <https://arxiv.org/abs/2210.02747>.
- Lipman, Y., Havasi, M., Holderrieth, P., Shaul, N., Le, M., Karrer, B., Chen, R. T. Q., Lopez-Paz, D., Ben-Hamu, H., and Gat, I. Flow matching guide and code, 2024. URL <https://arxiv.org/abs/2412.06264>.
- Liu, A., Sap, M., Lu, X., Swayamdipta, S., Bhagavatula, C., Smith, N. A., and Choi, Y. DExperts: Decoding-time controlled text generation with experts and anti-experts. In Zong, C., Xia, F., Li, W., and Navigli, R. (eds.), *Proceedings of the 59th Annual Meeting of the Association for Computational Linguistics and the 11th International Joint Conference on Natural Language Processing (Volume 1: Long Papers)*, pp. 6691–6706, Online, August 2021. Association for Computational Linguistics. doi: 10.18653/v1/2021.acl-long.522. URL <https://aclanthology.org/2021.acl-long.522/>.
- Lou, A., Meng, C., and Ermon, S. Discrete diffusion language modeling by estimating the ratios of the data distribution, 2024. URL <https://openreview.net/forum?id=7lmqtQdKB9>.
- Martino, L., Elvira, V., and Louzada, F. Weighting a resampled particle in sequential monte carlo. In *2016 IEEE Statistical Signal Processing Workshop (SSP)*, pp. 1–5, 2016. doi: 10.1109/SSP.2016.7551711.
- Nisonoff, H., Xiong, J., Allenspach, S., and Listgarten, J. Unlocking guidance for discrete state-space diffusion and flow models, 2024. URL <https://arxiv.org/abs/2406.01572>.
- Podell, D., English, Z., Lacey, K., Blattmann, A., Dockhorn, T., Müller, J., Penna, J., and Rombach, R. Sdxl: Improving latent diffusion models for high-resolution image synthesis, 2023. URL <https://arxiv.org/abs/2307.01952>.
- Rombach, R., Blattmann, A., Lorenz, D., Esser, P., and Ommer, B. High-resolution image synthesis with latent diffusion models, 2022. URL <https://arxiv.org/abs/2112.10752>.
- Ronneberger, O., Fischer, P., and Brox, T. U-net: Convolutional networks for biomedical image segmentation, 2015. URL <https://arxiv.org/abs/1505.04597>.
- Shi, J., Han, K., Wang, Z., Doucet, A., and Titsias, M. Simplified and generalized masked diffusion for discrete data. In *The Thirty-eighth Annual Conference on Neural Information Processing Systems*, 2024. URL <https://openreview.net/forum?id=xcqSOfHt4g>.
- Song, Y. and Ermon, S. Generative modeling by estimating gradients of the data distribution, 2020. URL <https://arxiv.org/abs/1907.05600>.
- Song, Y., Sohl-Dickstein, J., Kingma, D. P., Kumar, A., Ermon, S., and Poole, B. Score-based generative modeling through stochastic differential equations, 2021. URL <https://arxiv.org/abs/2011.13456>.
- Uehara, M., Zhao, Y., Wang, C., Li, X., Regev, A., Levine, S., and Biancalani, T. Inference-time alignment in diffusion models with reward-guided generation: Tutorial and review, 2025. URL <https://arxiv.org/abs/2501.09685>.
- Vargas, F., Grathwohl, W., and Doucet, A. Denoising diffusion samplers. *arXiv preprint arXiv:2302.13834*, 2023.
- Vargas, F., Nusken, N., Padhy, S., and Blessing, D. Transport meets variational inference: Controlled monte carlo diffusions. In *The Twelfth International Conference on Learning Representations: ICLR 2024*, 2024.

- Venkatraman, S., Jain, M., Scimeca, L., Kim, M., Sendera, M., Hasan, M., Rowe, L., Mittal, S., Lemos, P., Bengio, E., Adam, A., Rector-Brooks, J., Bengio, Y., Berseth, G., and Malkin, N. Amortizing intractable inference in diffusion models for vision, language, and control. In *The Thirty-eighth Annual Conference on Neural Information Processing Systems*, 2024. URL <https://openreview.net/forum?id=gVTkMsaaGI>.
- Vignac, C., Krawczuk, I., Siraudin, A., Wang, B., Cevher, V., and Frossard, P. Digress: Discrete denoising diffusion for graph generation. In *The Eleventh International Conference on Learning Representations*, 2023. URL <https://openreview.net/forum?id=UaAD-Nu86WX>.
- Watson, J. L., Juergens, D., Bennett, N. R., Trippe, B. L., Yim, J., Eisenach, H. E., Ahern, W., Borst, A. J., Ragotte, R. J., Milles, L. F., et al. De novo design of protein structure and function with rfdiffusion. *Nature*, 620(7976): 1089–1100, 2023.
- Wu, L., Trippe, B., Naesseth, C., Blei, D., and Cunningham, J. P. Practical and asymptotically exact conditional sampling in diffusion models. *Advances in Neural Information Processing Systems*, 36, 2024.
- Wu, Y., Schuster, M., Chen, Z., Le, Q. V., Norouzi, M., Macherey, W., Krikun, M., Cao, Y., Gao, Q., Macherey, K., Klingner, J., Shah, A., Johnson, M., Liu, X., Łukasz Kaiser, Gouws, S., Kato, Y., Kudo, T., Kazawa, H., Stevens, K., Kurian, G., Patil, N., Wang, W., Young, C., Smith, J., Riesa, J., Rudnick, A., Vinyals, O., Corrado, G., Hughes, M., and Dean, J. Google’s neural machine translation system: Bridging the gap between human and machine translation, 2016. URL <https://arxiv.org/abs/1609.08144>.
- Zhang*, T., Kishore*, V., Wu*, F., Weinberger, K. Q., and Artzi, Y. Bertscore: Evaluating text generation with bert. In *International Conference on Learning Representations*, 2020. URL <https://openreview.net/forum?id=SkeHuCVFDr>.

A. Related work

Diffusion models have emerged as a powerful class of generative models that can be interpreted through various theoretical frameworks, including score-based modeling (Song & Ermon, 2020; Song et al., 2021), flow matching (Lipman et al., 2023; 2024), variational methods (Ho et al., 2020) and stochastic interpolant (Albergo & Vanden-Eijnden, 2023; Albergo et al., 2023). Their versatility has led to successful applications across diverse domains, from image and video generation (Rombach et al., 2022; Podell et al., 2023; Blattmann et al., 2023) to molecular design (Cornet et al., 2024; Vignac et al., 2023; Hoogeboom et al., 2022), protein design (Watson et al., 2023), and text generation (Shi et al., 2024; Lou et al., 2024; Gulrajani & Hashimoto, 2023), where controlled generation is often crucial.

Two primary approaches have been developed for controlled generation: classifier guidance (Dhariwal & Nichol, 2021) and classifier-free guidance (Ho & Salimans, 2022b). Classifier guidance incorporates gradients from a trained classifier to steer the generation process, while CFG eliminates the need for a separate classifier by jointly training conditional and unconditional models. For scenarios with limited data where training classifiers or conditional models is impractical, DEFT (Denker et al., 2024) demonstrates that fine-tuning a small network can learn classifier scores directly, enabling guidance of unconditional models. However, recent theoretical analyses (Chidambaram et al., 2024; Bradley & Nakkiran, 2024) have revealed fundamental limitations of guidance methods. Specifically, as the guidance temperature parameter increases to strengthen conditioning, these methods fail to sample from their intended tilted target distributions. This limitation is particularly relevant for applications requiring precise control over generated samples.

In the discrete setting, several approaches have been proposed to adapt guidance methods. Nisonoff et al. (2024) adapt Classifier Free Guidance, Vignac et al. (2023) use Taylor expansions to approximate guidance terms with a property-predicting regressor. Li et al. (2024) introduce SVDD, integrating value functions for reward-based sampling without fine-tuning. Kerby & Moon (2024) develop a training-free guidance framework for discrete data generation.

Recent works propose finetuning approaches using reinforcement learning to sample from tempered distributions (Domingo-Enrich et al., 2025; Venkatraman et al., 2024; Fan et al., 2023; Black et al., 2024; Clark et al., 2024; Uehara et al., 2025). Black et al. (2024) introduce Denoising Diffusion Policy Optimization (DDPO), which reformulates the denoising process as a multi-step decision problem. Clark et al. (2024) propose Direct Reward Fine-tuning (DRaFT), demonstrating that backpropagation through the entire sampling procedure can effectively optimize differentiable reward functions. Fan et al. (2023) develop DPOK, which combines policy optimization with KL regularization for fine-tuning text-to-image models, showing improvements in both image-text alignment and image quality compared to supervised fine-tuning approaches.

B. A Primer on Continuous-Time Markov Chains

B.1. Definition

A Continuous-Time Markov Chain $\{X_t\}_{t \in [0,1]}$ on finite state space $\mathcal{X} = \{1, \dots, |\mathcal{X}|\}$ is collection of time-indexed random variables taking values on \mathcal{X} . A CTMC $\{X_t\}_{t \in [0,1]}$ obeys the Markov property, that is, for all $A \subseteq \mathcal{X}$, $n \in \mathbb{N}$, $t_1, \dots, t_n \in [0, 1]$, and $0 \leq x_1 < \dots < x_n \leq 1 \in \mathcal{X}$:

$$\mathbb{P}(X_t \in A | X_{t_1} = x_1, \dots, X_{t_n} = x_n) = \mathbb{P}(X_t \in A | X_{t_n} = x_n). \quad (15)$$

The initial distribution $p_0(x_0)$ and transition probability $p_{t|s}(x_t|x_s)$ are defined as,

$$p_0(x_0) = \mathbb{P}(X_0 = x_0) \quad p_{t|s}(x_t|x_s) = \mathbb{P}(X_t = x_t, X_s = x_s). \quad (16)$$

Notably, a CTMC is **càdlàg** by convention, that is for every $t \geq 0$:

1. $\lim_{s \rightarrow t^+} X(s) = X(t)$ (right-continuous at t),
2. $\lim_{s \rightarrow t^-} X(s)$ exists (finite left-hand limit at t).

B.2. The Transition Rate Matrix

One way to characterise a CTMC is through the time-dependent **transition rate matrix** R_t (also known as the **generator**), defined as,

$$\forall x, y \in \mathcal{X}. R_t(x, y) = \lim_{\Delta t \rightarrow 0} \frac{p_{t+\Delta t|t}(x_{t+\Delta t}|x_t) - \delta_{x,y}}{\Delta t} \quad (17)$$

where $\delta_{a,b}$ is 1 if $a = b$ and 0 if otherwise.

By definition, a first-order approximation of the transition probability is:

$$p_{t+\Delta t|t}(x_{t+\Delta t}|x_t) = \delta_{x_t+\Delta t, x_t} + R_t(x_t, x_{t+\Delta t})\Delta t + o(\Delta t). \quad (18)$$

By noticing that $\sum_{y \in \mathcal{X}} p_{t+\Delta t|t}(y|x) = 1$, we derive the mass conservation property of R_t ,

$$R_t(x, x) = - \sum_{y \in \mathcal{X}: x \neq y} R_t(x, y) \quad (19)$$

By convention, we define $R_t(x)$ as,

$$R_t(x) = \sum_{y \in \mathcal{X}: x \neq y} R_t(x, y). \quad (20)$$

B.3. The Kolmogorov Equations

In this section, we outline both Kolmogorov Forward and Backward Equation that govern respectively the change of the probability mass, and expectations of some function over time.

Kolmogorov-Forward Equation. The Kolmogorov Forward Equation (or the continuity equation) governs the change of probability mass over time. It states that the probability mass p_t satisfies the following equation:

$$\forall 0 \leq t \leq 1. \partial_t p_t(x_t) = \underbrace{\sum_{y \in \mathcal{X}: x_t \neq y} R_t(y, x_t) p_t(y)}_{\text{incoming probability mass}} - \underbrace{\sum_{y \in \mathcal{X}: x_t \neq y} R_t(x_t, y) p_t(x_t)}_{\text{outgoing probability mass}} \quad (21)$$

In other words, the rate of change of probability mass equals the difference between incoming and outgoing probability flows. In matrix notation, this equation is:

$$\partial_t p_t = R_t^\top p_t \quad (22)$$

Kolmogorov Backward Equation Given a function $h : \mathcal{X} \rightarrow \mathbb{R}$, the Kolmogorov Backward Equation states that the function $u_t(x)$ defined as,

$$u_t(x) = \mathbb{E}[h(X_1)|X_t = x], \quad (23)$$

satisfies the ordinary differential equation,

$$\partial_t u_t(x) = - \sum_y R_t(x, y) u_t(y), \quad (24)$$

writing u_t as a column vector, this can be written in matrix form,

$$\partial_t u_t = -R_t^\top u_t. \quad (25)$$

B.4. Reverse-time CTMC

Time-reversed CTMC is a core concept of diffusion model. A reverse-time CTMC $\{Y_t\}_{t \in [0,1]}$ with time-dependent rate R_t is defined as $Y_t = \hat{Y}_{1-t}$ where $\{\hat{Y}_t\}_{t \in [0,1]}$ is a forward-time CTMC with transition rate R_{1-t} . The reverse-time Kolmogorov Equations are then obtained by applying a change of variable $t \mapsto 1 - t$.

C. Proof for Section 3

In this section, we prove Proposition 3.2.

Proposition 3.2. Let $M_t[q]$ denote the evolution of probability mass q up to time t under the corrupting process. Define $p_t^{\alpha, \text{true}}$ as:

$$p_t^{\alpha, \text{true}} = M_t[p_0(\cdot) p_0(\zeta|\cdot)^\alpha / \mathcal{Z}_\alpha].$$

Then,

$$p_t^{\alpha, \text{true}}(x_t) \propto p_t(x_t) \mathbb{E}[p_0(\zeta|X_0)^\alpha | X_t = x_t].$$

The true tempered rate matrix $R_t^{\alpha, \text{true}}$ given by:

$$\begin{aligned} \forall x \neq y, R_t^{\alpha, \text{true}}(x, y|\zeta) &= R_t(x, y) \frac{\mathbb{E}[p_0(\zeta|X_0)^\alpha | X_t=y]}{\mathbb{E}[p_0(\zeta|X_0)^\alpha | X_t=x]}, \\ \forall x, R_t^{\alpha, \text{true}}(x, x|\zeta) &= - \sum_{y \neq x} R_t^{\alpha, \text{true}}(x, y|\zeta), \end{aligned}$$

is time-reversal of the corruption process that stats from $p_0(\cdot) p_0(\zeta|\cdot)^\alpha / \mathcal{Z}_\alpha$

Proof. Recall that $\{X_t\}_{t \in [0,1]}$ is a reversed-time CTMC corresponding to the unconditional discrete diffusion model. Let $\{p_{t|s}^{\text{corrupt}}(x_t|x_s)\}_{t>s}$ and $\{p_{t|s}(x_t|x_s)\}_{t<s}$ be the transition probability of the forward-time corrupting process and reverse-time generative process. We first show $p_t^{\alpha}(x_t) \propto p_t(x_t) \mathbb{E}[p_0(\zeta|X_0)^\alpha | X_t = x_t]$. By definition,

$$p_t^{\alpha, \text{true}}(x_t) = M_t[p_0(\cdot) p(\zeta|\cdot)^\alpha / \mathcal{Z}_\alpha] \quad (26)$$

$$\propto \sum_{x_0} p_{t|0}^{\text{corrupt}}(x_t|x_0) p_0(x_0) p(\zeta|x_0)^\alpha \quad (27)$$

$$= \sum_{x_0} p_{0|t}(x_0|x_t) \frac{p_t(x_t)}{p_0(x_0)} p_0(x_0) p(\zeta|x_0)^\alpha \quad (28)$$

$$= p_t(x_t) \sum_{x_0} p_{0|t}(x_0|x_t) p(\zeta|x_0)^\alpha \quad (29)$$

$$= p_t(x_t) \mathbb{E}[p(\zeta|X_0)^\alpha | X_t = x_t]. \quad (30)$$

Then it follow from standard results of time-reversal of the CTMC such as that in (Lou et al., 2024), the rate matrix of the time-reversal can be written as:

$$\forall x \neq y. R_t^{\alpha, \text{true}}(x, y|\zeta) = R_t(x, y) \frac{p_t^{\alpha, \text{true}}(y)}{p_t^{\alpha, \text{true}}(x)} = R_t^{\alpha, \text{true}}(x, y|\zeta) = R_t(x, y) \frac{\mathbb{E}[p_0(\zeta|X_0)^\alpha | X_t=y]}{\mathbb{E}[p_0(\zeta|X_0)^\alpha | X_t=x]} \quad (31)$$

□

D. Proof of Proposition 4.1

Proposition 4.1. Let proposal $\{Y_t\}_{t \in [0,1]}$ be reverse-time CTMC with rate matrix Q_t and initial distribution $p_1(\cdot)$. Define $\{W_t\}_{t \in [0,1]}$ by

$$W_t = \frac{d\mathbb{P}_t^{\text{base}}}{d\mathbb{Q}_t} \left(\frac{d\mathbb{P}_t^{\alpha=1}}{d\mathbb{P}_t^{\text{base}}} \right)^\alpha,$$

where we have $\mathbb{P}_t^{\text{base}} = \text{Law}\{X_\tau\}_{\tau \in [t,1]}$, $\mathbb{P}^{\alpha=1} = \text{Law}\{X_\tau | \zeta\}_{\tau \in [t,1]}$, $\mathbb{Q} = \text{Law}\{Y_\tau\}_{\tau \in [t,1]}$. Then,

$$\ln \frac{d\mathbb{P}_t^{\text{base}}}{d\mathbb{Q}_t} = \sum_{\substack{\tau \geq t \\ Y_{\tau+} \neq Y_\tau}} \ln R_t(Y_{\tau+}, Y_\tau) - \ln Q_t(Y_{\tau+}, Y_{s_\tau}) + \int_1^t Q_\tau(Y_t) - R_\tau(Y_t) d\tau$$

and

$$\ln \frac{d\mathbb{P}_t^{\alpha=1}}{d\mathbb{P}_t^{\text{base}}} = \sum_{\substack{\tau \geq t \\ Y_{\tau+} \neq Y_\tau}} \ln R_t^{\alpha=1}(Y_{\tau+}, Y_\tau | \zeta) - \ln R_t(Y_{\tau+}, Y_\tau) + \int_1^t R_\tau(Y_\tau) - R_\tau^{\alpha=1}(Y_\tau | \zeta) d\tau.$$

For any p_t^α -integrable function h and time $t \in [0, 1]$,

$$\mathbb{E}_{x \sim p_t^\alpha} [h(x)] = \frac{\mathbb{E}[W_t \cdot h(Y_t)]}{\mathbb{E}[W_t]}.$$

Proof. Via the Radon-Nikodym Theorem, we seek to compute the importance weight (i.e. the Radon-Nikodym derivative ²)

$$\frac{d\mathbb{P}_t^\alpha}{d\mathbb{Q}_t} = \frac{d\mathbb{P}_t^{\text{base}}}{d\mathbb{Q}_t} \cdot \frac{d\mathbb{P}_t^\alpha}{d\mathbb{P}_t^{\text{base}}} = \frac{d\mathbb{P}_t^{\text{base}}}{d\mathbb{Q}_t} \cdot p_t(\zeta | Y_t)^\alpha, \quad (32)$$

where $\frac{d\mathbb{P}_t^\alpha}{d\mathbb{P}_t^{\text{base}}} = p_t(\zeta | Y_t)^\alpha$ follows by construction of \mathbb{P}_t^α and a direct application of the disintegration theorem (Léonard, 2014) (i.e. the product rule), then considering $\alpha = 1$ it follows that $p_t(\zeta | Y_t)^\alpha = \left(\frac{d\mathbb{P}_t^{\alpha=1}}{d\mathbb{P}_t^{\text{base}}} \right)^\alpha$, and thus the importance weights between our proposal and the tilted path measure reduce to:

$$W_t = \frac{d\mathbb{P}_t^\alpha}{d\mathbb{Q}_t} = \frac{d\mathbb{P}_t^{\text{base}}}{d\mathbb{Q}_t} \left(\frac{d\mathbb{P}_t^{\alpha=1}}{d\mathbb{P}_t^{\text{base}_t}} \right)^\alpha, \quad (33)$$

Finally, the Radon-Nikodym derivative between two arbitrary reverse-time CTMC path measures \mathbb{P}'_t and \mathbb{Q}'_t with transition rate matrix R'_τ and Q'_τ evaluated at the path Y , is known to be the following Appendix C.1 of (Campbell et al., 2024), that is,

$$\frac{d\mathbb{P}'_t}{d\mathbb{Q}'_t} = \frac{\exp(-\int_1^t R'_\tau(Y_t) d\tau)}{\exp(-\int_1^t Q'_\tau(Y_t) d\tau)} \prod_{\substack{\tau \geq t \\ Y_{\tau+} \neq Y_\tau}} \frac{R'_\tau(Y_{\tau+}, Y_\tau)}{Q'_\tau(Y_{\tau+}, Y_\tau)} \quad (34)$$

We refer the readers to (Campbell et al., 2024) for an accessible sketch of this result, which follows (Del Moral & Penev, 2017). Then, substituting Equation 34 into the RNDs of Equation 33 concludes the proof. \square

D.1. Itô Process Counterpart

The core result in Proposition 4.1 is in noticing that $p_t(\zeta | Y_t)^\alpha = \left(\frac{d\mathbb{P}_t^{\alpha=1}}{d\mathbb{P}_t^{\text{base}}} \right)^\alpha$ and decomposing the IS weight via the chain rule and applying Girsanovs Theorem.

Due to the very modular nature of our result our proposition seamlessly extends to Stochastic Differential Equations.

Proposition D.1. *Let proposal $\{Y_t\}_{t \in [0,1]}$ be a reverse-time SDE with drift $b_t(x)$, diffusion coefficient g_t and initial distribution $p_1(\cdot)$ and X_t also be a reverse-time SDE with drift f_t , diffusion coefficient g_t and initial distribution $p_1(\cdot)$. Define $\{W_t\}_{t \in [0,1]}$ by*

$$W_t = \frac{d\mathbb{P}_t^{\text{base}}}{d\mathbb{Q}_t} \left(\frac{d\mathbb{P}_t^{\alpha=1}}{d\mathbb{P}_t^{\text{base}}} \right)^\alpha, \quad (35)$$

where we have $\mathbb{P}_t^{\text{base}} = \text{Law}\{X_\tau\}_{\tau \in [t,1]}$, $\mathbb{P}^{\alpha=1} = \text{Law}\{X_\tau | \zeta\}_{\tau \in [t,1]}$, $\mathbb{Q} = \text{Law}\{Y_\tau^{b,p_1}\}_{\tau \in [t,1]}$. Then,

$$\ln \frac{d\mathbb{P}_t^{\text{base}}}{d\mathbb{Q}_t} = \int_t^1 \frac{1}{g_\tau^2} (f_\tau(Y_\tau) - b_\tau(Y_\tau))^\top \overleftarrow{d} Y_\tau + \int_t^1 \frac{1}{2g_\tau^2} (\|f_\tau(Y_\tau)\|^2 - \|b_\tau(Y_\tau)\|^2) d\tau$$

²We consider all RND's evaluated at Y_t that is when we write $\frac{d\mathbb{P}'_t}{d\mathbb{Q}'_t}$ it is short for $\frac{d\mathbb{P}'_t}{d\mathbb{Q}'_t}(Y_t)$.

and

$$\ln \frac{d\mathbb{P}_t^{\alpha=1}}{d\mathbb{P}_t^{\text{base}}} = \int_t^1 \frac{1}{g_\tau^2} (f_\tau^{\cdot|\zeta}(Y_\tau) - f_\tau(Y_\tau))^\top \overleftarrow{d} Y_\tau + \int_t^1 \frac{1}{2g_\tau^2} (\|f_\tau^{\cdot|\zeta}(Y_\tau)\|^2 - \|f_\tau(Y_\tau)\|^2) d\tau$$

Where $f_\tau^{\cdot|\zeta}(y_\tau) = f_\tau(y_\tau) - g_\tau^2 \nabla \ln p_\tau(\zeta|y_\tau)$ as per (Denker et al., 2024, Proposition 2.2).

For any p_t^α -integrable function h and time $t \in [0, 1]$,

$$\mathbb{E}_{x \sim p_t^\alpha} [h(x)] = \frac{\mathbb{E}[W_t \cdot h(Y_t)]}{\mathbb{E}[W_t]}.$$

Proof. Equation 35 follows directly from Proposition 4.1. Then, for the RNDs between two reverse time SDEs, we use Equation 64 in (Vargas et al., 2024). Note for the VP-SDE case; these expressions can be simplified further as done in (Vargas et al., 2023, Equation 9). Note as with the rest of our results, we require that $p_1(y_1|\zeta) = p_1(y_1)$ which is approximately true in the limit for VP-SDE as $p_1(\cdot|\zeta) \approx \mathcal{N}(0, I)$. \square

D.2. Alternative Proof of Proposition 4.1 without Radon-Nikodym Theorem

In this appendix, we present an equivalent statement of Proposition 4.1 and a proof that does not rely on the Radon-Nikodym Theorem.

Proposition 4.1. Let proposal $\{Y_t\}_{t \in [0,1]}$ be a reverse-time CTMC with rate matrix Q_t and initial distribution $p_1(\cdot)$. Define $\{W_t\}_{t \in [0,1]}$ by,

$$\begin{aligned} W_t &= \exp(A_t), \\ A_0 &= 0, \\ A_t &= \sum_{\substack{t \leq \tau \\ Y_{\tau+} \neq Y_\tau}} [\ln R_\tau(Y_{\tau+}, Y_\tau) - \ln Q_\tau(Y_{\tau+}, Y_\tau)] + \sum_{\substack{t \leq \tau \\ Y_{\tau+} \neq Y_\tau}} \alpha \ln(R_\tau^{\alpha=1}(Y_{\tau+}, Y_\tau|\zeta)/R_\tau(Y_{\tau+}, Y_\tau)) \\ &\quad + \int_1^t [Q_\tau(Y_t) - R_\tau(Y_t) + \alpha R_\tau(Y_t|\zeta) - \alpha R_\tau^{\alpha=1}(Y_t|\zeta)] d\tau. \end{aligned}$$

For any p_t -integrable function h and time $t \in [0, 1]$,

$$\mathbb{E}_{x \sim p_t^\alpha} [h(x)] = \frac{\mathbb{E}[W_t \cdot h(Y_t)]}{\mathbb{E}[W_t]}.$$

where the expectation is taken over the law of (Y_t, W_t) .

Proof. We closely follow the sketches of (Carbone et al., 2023; Albergo & Vanden-Eijnden, 2024). Assume $p_1(x_1) = p_1(x_1|\zeta)$. We first show that the coupled system (Y_t, A_t) with A_t defined as,

$$W_0 = 0 \tag{36}$$

$$A_t = \sum_{\substack{t \leq \tau \\ Y_{\tau+} \neq Y_\tau}} [\ln R_t(Y_{\tau+}, Y_\tau) - \ln Q_t(Y_{\tau+}, Y_\tau)] + \sum_{\substack{t \leq \tau \\ Y_{\tau+} \neq Y_\tau}} \alpha [\ln p_t(\zeta|Y_\tau) - \ln p_t(\zeta|Y_{\tau+})] \tag{37}$$

$$+ \int_1^t [R_\tau(Y_t) - Q_\tau(Y_t) - \alpha \partial_t \ln p_t(\zeta|Y_t)] d\tau, \tag{38}$$

satisfies,

$$\mathbb{E}_{x \sim p_t^\alpha} [h(x)] = \frac{\mathbb{E}[e^{A_t} h(Y_t)]}{\mathbb{E}[e^{A_t}]}, \tag{39}$$

Write $\Delta A_t(x, y) = \ln R_t(x, y) - \ln Q_t(x, y) + \alpha(\ln p_t(\zeta|y) - \ln p_t(\zeta|x))$. Define $f_t(y, a)$ to be the joint density of (Y_t, A_t) , the joint density is governed by the (reverse-time) continuity equation,

$$\begin{aligned} \partial_t f_t(y, a) &= - \left[\sum_{z \neq y} Q_t(z, y) f_t(z, a - \Delta A(z, y)) - f_t(y, a) Q_t(y) + [Q_t(y) - R_t(y) - \alpha \partial_t \ln p_t(\zeta|y)] \partial_a f_t(y, a) \right], \\ f_1(y, a) &= \delta(a) p_1(x_1) \end{aligned} \quad (40)$$

□

Define $g_t(y) = \int_{\mathbb{R}} e^a f_t(y, a) da$. Then, via dominated convergence theorem (i.e. $\partial_t g_t(y) = \int_{\mathbb{R}} e^a \partial_t f_t(y, a) da$) and substituting $\partial_t f_t(y, a)$ from Equation 40, it follows that

$$\partial_t g_t(y) = \int_{\mathbb{R}} e^a \sum_{z \neq y} Q_t(z, y) f_t(z, a - \Delta A(z, y)) da \quad (41)$$

By a change of variable $a' = a - \Delta A(z, y)$, then,

$$\int_{\mathbb{R}} e^a \sum_{z \neq y} Q_t(z, y) f_t(z, a - \Delta A(z, y)) da = \int_{\mathbb{R}} e^{a'} \sum_{z \neq y} e^{\Delta A(z, y)} Q_t(z, y) f_t(z, a') da' \quad (42)$$

$$= \sum_{z \neq y} R_t(z, y) \cdot \frac{p_t(\zeta|y)^\alpha}{p_t(\zeta|z)^\alpha} \cdot g_t(z) \quad (43)$$

And finally, by integration by parts, and noting that $\int_{\mathbb{R}} e^a f_t(y, a) da = Q_t(y) g_t(y)$, we have

$$\int_{\mathbb{R}} e^a [Q_t(y) - R_t(y) + \alpha \partial_t \ln p_t(\zeta|y)] \partial_a f_t(y, a) da = [Q_t(y) - R_t(y) - \alpha \partial_t \ln p_t(\zeta|y)] g_t(y). \quad (44)$$

Combining the three cases, we have:

$$g_1(y) = p_1(y) \quad (45)$$

$$\partial_t g_t(y) = - \left[\sum_{z \neq y} R_t(z, y) \cdot \frac{p_t(\zeta|y)^\alpha}{p_t(\zeta|z)^\alpha} \cdot g_t(z) - Q_t(y) g_t(y) + [Q_t(y) - R_t(y) - \alpha \partial_t \ln p_t(\zeta|y)] g_t(y) \right]. \quad (46)$$

$$(47)$$

Notice that g reduces to a system of ODEs and thus, by the Picard-Lindelöf theorem, has a unique solution. Recall that $\mathcal{Z}_1^\alpha = \sum_x p_1(x) p_1(\zeta|x)^\alpha = p(\zeta)^\alpha$, writing $p(\zeta)$ as the density of ζ . Substituting $g_t(y) = p_t(y) \cdot p_t(\zeta|y)^\alpha / \mathcal{Z}_1^\alpha$, then,

$$\text{L.H.S} = \partial_t g(y) \quad (48)$$

$$= \frac{1}{\mathcal{Z}_1^\alpha} [p_t(\zeta|y)^\alpha \partial_t p_t(y) + p_t(y) \partial_t (p_t(\zeta|y)^\alpha)] \quad (49)$$

$$\text{R.H.S} = - \frac{1}{\mathcal{Z}_1^\alpha} \left[\sum_{z \neq y} R_t(z, y) \cdot \frac{p_t(\zeta|y)^\alpha}{p_t(\zeta|z)^\alpha} \cdot g_t(z) - Q_t(y) g_t(y) + [Q_t(y) - R_t(y) - \alpha \partial_t \ln p_t(\zeta|y)] g_t(y) \right] \quad (50)$$

$$= - \frac{1}{\mathcal{Z}_1^\alpha} \left[p_t(\zeta|y)^\alpha \sum_{z \neq y} R_t(z, y) p_t(z) - p_t(\zeta|y)^\alpha \sum_{z \neq y} R_t(y, z) p_t(y) - \alpha \partial_t \ln p_t(\zeta|y) p_t(y) p_t(\zeta|y)^\alpha \right] \quad (51)$$

$$= \frac{1}{\mathcal{Z}_1^\alpha} [p_t(\zeta|y)^\alpha \partial_t p_t(y) + p_t(y) \partial_t (p_t(\zeta|y)^\alpha)] \quad (52)$$

$$= \text{L.H.S} \quad (53)$$

Since $p_1(y) = p_1(y | \zeta)$, it follows that the boundary condition $g_1(y) = p_1(y)$ is fulfilled. Then,

$$\mathbb{E}[e^{A_t}] = \sum_x \int_{\mathbb{R}} e^a f_t(x, a) da = \sum_x g_t(x) = \sum_x p_t(x) p_t(\zeta | x)^\alpha / \mathcal{Z}_1^\alpha = \mathcal{Z}_t^\alpha / \mathcal{Z}_1^\alpha \quad (54)$$

Similarly, for an arbitrary function h if we define $g_t^h(x) = \int_{\mathbb{R}} e^a h(x) f_t(x, a) da$, we may show that

$$\mathbb{E}[e^{A_t} h(x)] = \sum_x \int_{\mathbb{R}} e^a h(x) f_t(x, a) da = \sum_x h(x) p_t(x) p_t(\zeta | x)^\alpha / \mathcal{Z}_1^\alpha. \quad (55)$$

Combining the two equations, we have,

$$\frac{\mathbb{E}[e^{A_t} h(x)]}{\mathbb{E}[e^{A_t}]} = \frac{1}{\mathcal{Z}_t^\alpha} \sum_x h(x) p_t(x) p_t(\zeta | x)^\alpha, \quad (56)$$

as desired.

To finish off the proof, we show that following:

1. $\forall x \neq y. \alpha(\ln p_t(\zeta | y) - \ln p_t(\zeta | x)) = \alpha(\ln R_t^{\alpha=1}(x, y) - \ln R_t(x, y))$
2. $\partial_t \ln p_t(\zeta | x_t) = \alpha R_t^{\alpha=1}(x) - \alpha R_t(x)$

The first equation follows from the definition of the guided ratio matrix $R_t^{\alpha=1}(x)$. To show that $\partial_t \ln p_t(\zeta | x_t) = \alpha R_t(x) - \alpha R_t^{\alpha=1}(x)$, recall,

$$p_t(\zeta | x_t) = \mathbb{E}[p_t(\zeta | X_0) | X_t = x_t], \quad (57)$$

Therefore,

$$\partial_t \ln p_t(\zeta | x_t) = \frac{1}{p_t(\zeta | x_t)} \partial_t p_t(\zeta | x_t) \quad (58)$$

$$= \frac{1}{p_t(\zeta | x_t)} \sum_y R_t(x_t, y) p_t(\zeta | y) \quad \text{(Reverse-Time) Kolmogorov Backward Equation} \quad (59)$$

$$= R_t^{\alpha=1}(x_t) - R_t(x_t) \quad \text{Definition of } R_t^{\alpha=1} \quad (60)$$

This concludes the proof.

E. Statement and Derivation of Discretised Weights

In this appendix, we show a discrete time version of Proposition 4.1 and the proof.

Proposition E.1. Define $\{\hat{W}_{t_k}\}_{k \in \{1, \dots, T\}}$ as:

$$\begin{aligned} \hat{W}_0 &= 1, \\ \hat{W}_{t_k} &= \prod_{1 \leq j < k} \frac{p_{t_{j+1}|t_j}(Y_{t_{j+1}} | Y_{t_j})}{q_{t_{j+1}|t_j}(Y_{t_{j+1}} | Y_{t_j})} \\ &\quad \cdot \prod_{1 \leq j < k} \left[\frac{p_{t_{j+1}|t_j}(Y_{t_{j+1}} | Y_{t_j}, \zeta)}{p_{t_{j+1}|t_j}(Y_{t_{j+1}} | Y_{t_j})} \right]^\alpha. \end{aligned}$$

If $p_1(x_1) = p_1(x_1 | \zeta)$, then for any function $h : \mathcal{X} \rightarrow \mathbb{R}$ and $k \in \{1, \dots, T\}$,

$$\frac{1}{\mathcal{Z}_{t_k}^\alpha} \sum_x h(x) p_{t_k}(x) p_{t_k}(\zeta | x)^\alpha = \frac{\mathbb{E}[\hat{W}_{t_k} h(Y_{t_k})]}{\mathbb{E}[\hat{W}_{t_k}]},$$

where the expectation is taken over the law of (Y_t, \hat{W}_t) .

Proof. First note that,

$$p_{t_{j+1}|t_j}(Y_{t_{j+1}}|Y_{t_j}, \zeta) = p_{t_j|t_{j+1}}^{\text{corrupt}}(Y_{t_j}|Y_{t_{j+1}}) \frac{M_t[p_0(x_0|\zeta)](Y_{t_{j+1}})}{M_t[p_0(x_0|\zeta)](Y_{t_j})} \quad (61)$$

$$= p_{t_j|t_{j+1}}^{\text{corrupt}}(Y_{t_j}|Y_{t_{j+1}}) \frac{p_t(Y_{t_{j+1}})p_t(\zeta|Y_{t_{j+1}})}{p_t(Y_{t_j})p_t(\zeta|Y_{t_j})} \quad (62)$$

$$= p_{t_{j+1}|t_j}(Y_{t_{j+1}}|Y_{t_j}) \frac{p_t(\zeta|Y_{t_{j+1}})}{p_t(\zeta|Y_{t_j})}. \quad (63)$$

Then it follows that,

$$\hat{W}_{t_k} = \prod_{1 \leq j < k} \frac{p_{t_{j+1}|t_j}(Y_{t_{j+1}}|Y_{t_j})}{q_{t_{j+1}|t_j}(Y_{t_{j+1}}|Y_{t_j})} \prod_{1 \leq j < k} \left[\frac{p_t(\zeta|Y_{t_{j+1}})}{p_t(\zeta|Y_{t_j})} \right]^\alpha \quad (64)$$

$$= \prod_{1 \leq j < k} \frac{p_{t_{j+1}|t_j}(Y_{t_{j+1}}|Y_{t_j})}{q_{t_{j+1}|t_j}(Y_{t_{j+1}}|Y_{t_j})} \left[\frac{p_{t_k}(\zeta|Y_{t_k})}{p_1(\zeta|Y_1)} \right]^\alpha \quad (65)$$

$$= \prod_{1 \leq j < k} \frac{p_{t_{j+1}|t_j}(Y_{t_{j+1}}|Y_{t_j})}{q_{t_{j+1}|t_j}(Y_{t_{j+1}}|Y_{t_j})} \left[\frac{p_{t_k}(\zeta|Y_{t_k})}{p(\zeta)} \right]^\alpha \quad Y_1 = X_1 \perp \zeta \quad (66)$$

$$= \frac{1}{Z_1^\alpha} \prod_{1 \leq j < k} \frac{p_{t_{j+1}|t_j}(Y_{t_{j+1}}|Y_{t_j})}{q_{t_{j+1}|t_j}(Y_{t_{j+1}}|Y_{t_j})} \quad Z_1^\alpha [p_{t_k}(\zeta|Y_{t_k})]^\alpha = \sum_x p_1(x) p_1(\zeta|x)^\alpha = p(\zeta)^\alpha. \quad (67)$$

Then,

$$\begin{aligned} \mathbb{E} \left[\hat{W}_{t_k} h(Y_{t_k}) \right] &= \sum_{Y_{t_k}} \hat{W}_{t_k} h(Y_{t_k}) q_{t_k}(Y_{t_k}) \\ &= \frac{1}{Z_1^\alpha} \sum_{\{y_i\}_{i=1}^k : y_k = Y_{t_k}} \hat{W}_{t_k} h(Y_{t_k}) \prod_{j=1}^{k-1} q_1(y_1) q_{t_{j+1}|t_j}(y_{t_{j+1}}|y_{t_j}) \\ &= \frac{1}{Z_1^\alpha} \sum_{\{x_i\}_{i=1}^k : x_k = Y_{t_k}} h(Y_{t_k}) p_t(\zeta|Y_{t_k})^\alpha q_1(x_1) \prod_{j=1}^{k-1} p_{t_{j+1}|t_j}(x_{t_{j+1}}|x_{t_j}) \\ &= \frac{1}{Z_1^\alpha} \sum_{Y_{t_k}} h(Y_{t_k}) p_t(\zeta|Y_{t_k})^\alpha p_t(Y_k) \end{aligned} \quad \text{Both } Y_t \text{ and } X_t \text{ starts at } p_1$$

Similarly,

$$\mathbb{E} \left[\hat{W}_{t_k} h(Y_{t_k}) \right] = Z_t^\alpha / Z_1^\alpha. \quad (68)$$

Combining the two equation lends us to,

$$\frac{1}{Z_{t_k}^\alpha} \sum_x h(x) p_{t_k}(x) p_{t_k}(\zeta|x)^\alpha = \frac{\mathbb{E} \left[\hat{W}_{t_k} h(Y_{t_k}) \right]}{\mathbb{E} \left[\hat{W}_{t_k} \right]} \quad (69)$$

This concludes the proof. \square

F. Sampling with Approximate Transition Discretised Weight

The exact transition probabilities $p_{t_{j+1}|t_j}$ and $q_{t_{j+1}|t_j}$ is typically unknown. In practice, we approximate these transitions using numerical methods such as Euler sampling. As the time step Δt approaches zero, these approximations converge to the true weights W_t . In Algorithm 2, we show the pseudocode of Algorithm 1 using the approximated transition probability $\tilde{q}_{t|s}$ and $\tilde{p}_{t|s}$.

Algorithm 2 Main Algorithm with Approximate Transition

Require: Number of particles K ; Approximate Proposal Transition $\tilde{q}_{t|s}$; Approximate transition $\tilde{p}_{t|s}$; Temperature α ; Time-grid $\{t_l\}_{l=1}^T$; ESS threshold ESS_THRESHOLD; Resampling algorithm `resample`.

- 1: **Initialisation:**
 - 2: Sample $\{x_1^{(i)}\}_{i=1}^K$ i.i.d. from p_1 .
 - 3: Set $\hat{w}_1^{(i)} \leftarrow 1$ for $i = 1, \dots, K$.
 - 4: **for** $l = 1$ to T **do**
 - 5: **for** $i = 1$ to K **do**
 - 6: {Step 1: Propagate}
 - 7: Sample $x_{l+1}^{(i)} \sim \tilde{q}_{t_{l+1}|t_l}(\cdot | x_l^{(i)})$
 - 8: {Step 2: Update and Normalize Weights}
 - 9: Set $\hat{w}_{l+1}^{(i)} \leftarrow \hat{w}_l^{(i)} \cdot \frac{\tilde{p}_{t_{l+1}|t_l}(x_{l+1}^{(i)} | x_l^{(i)})}{\tilde{q}_{t_{l+1}|t_l}(x_{l+1}^{(i)} | x_l^{(i)})} \cdot \left[\frac{\tilde{p}_{t_{l+1}|t_l}(x_{l+1}^{(i)} | x_l^{(i)}, \zeta)}{\tilde{p}_{t_{l+1}|t_l}(x_{l+1}^{(i)} | x_l^{(i)})} \right]^\alpha$
 - 10: **end for**
 - 11: {Step 3: Resample; see Appendix G for other resampling algorithms}
 - 12: Set $\text{ESS} \leftarrow \left(\sum_{i=1}^K \hat{w}_l^{(i)} \right)^2 / \sum_{i=1}^K (\hat{w}_l^{(i)})^2$
 - 13: **if** $\text{ESS} \leq \text{ESS_THRESHOLD}$ **then**
 - 14: $\tilde{w}_l^{(i)} \leftarrow \hat{w}_l^{(i)} / \sum_i \hat{w}_l^{(i)}$
 - 15: Set $x_{l+1}^{(i)}, \hat{w}_{l+1}^{(i)} \leftarrow \text{resample}(\{x_l^{(i)}\}, \{\tilde{w}_l^{(i)}\})$
 - 16: **end if**
 - 17: **end for**
 - 18: **Output:**
 - 19: Particles $\{x_T^{(i)}\}_{i=1}^K$
-

G. Pseudocode for Resampling Algorithms

In this section, we introduce various resampling strategies for Sequential Monte Carlo methods. Ultimately, the goal of resampling algorithm is to replace low weighted particles with high weighted particles to reduce the variance of weights such that the expectation of any function ϕ remains unchanged.

More specifically, consider at iteration l of a SMC algorithm, given K particles $\{x_l^{(i)}\}_{i=1}^K$ and $\{w_l^{(i)}\}_{i=1}^K$ from some joint distribution \mathbb{Q} induced by the SMC algorithm. A resampling algorithm returning $\{\tilde{x}^{(i)}\}_{i=1}^K$ and $\{\tilde{w}^{(i)}\}_{i=1}^K$ generates consistent samples as long as for any bounded and continuous function ϕ , $\mathbb{E}^{\mathbb{Q}}[w^{(i)}\phi(x^{(i)})] = \mathbb{E}^{\mathbb{Q}}[\tilde{w}^{(i)}\phi(\tilde{x}^{(i)})]$ where $\mathbb{E}^{\mathbb{Q}}$ notes an expectation on \mathbb{Q} .

G.1. Multinomial Resampling

The simplest and most common resampling strategy is the multinomial resampling, which involves the particles in the next iteration independently following a categorical distributions distributed according to the normalised weights.

Algorithm 3 Multinomial Resampling

Require: Number of Particles K ; Particles $\{x^{(i)}\}_{i=1}^K$; Normalised Weights $\{w^{(i)}\}_{i=1}^K$

- 1: **for** $i = 1$ to K **do**
 - 2: Sample $\tilde{x}^{(i)} \sim \sum_{j=1}^K w^{(j)}\delta_{x^{(j)}}(dx)$
 - 3: $\tilde{w}^{(i)} = 1/K$
 - 4: **end for**
 - 5: **Output:**
 - 6: Particles $\{\tilde{x}^{(i)}\}_{i=1}^K$ and Weights $\{\tilde{w}^{(i)}\}_{i=1}^K$
-

G.2. Partial Resampling

We further consider employing a partial resampling strategy adapted from (Martino et al., 2016), which we found to prevent mode collapse of samples effectively.

Algorithm 4 Partial Resampling

Require: Number of Particles K ; Particles $\{x^{(i)}\}_{i=1}^K$; Normalised Weights $\{w^{(i)}\}_{i=1}^K$; Resample Size M

- 1: Set Resample Indices $I = \{i|w^{(i)} \text{ among the } \lfloor M/2 \rfloor \text{ highest or } \lceil M/2 \rceil \text{ lowest}\}$
 - 2: **for** $i = 1$ to K **do**
 - 3: **if** $i \in I$ **then**
 - 4: Sample $\tilde{x}^{(i)} \sim \sum_{j=1}^K w^{(j)}\delta_{x^{(j)}}(dx)$
 - 5: Set $\tilde{w}^{(i)} \leftarrow 1/M \sum_{i \in I} w^{(i)}$
 - 6: **else**
 - 7: Set $\tilde{x}^{(i)} \leftarrow x^{(i)}$
 - 8: Set $\tilde{w}^{(i)} \leftarrow w^{(i)}$
 - 9: **end if**
 - 10: **end for**
 - 11: **Output:**
 - 12: Particles $\{\tilde{x}^{(i)}\}_{i=1}^K$ and Weights $\{\tilde{w}^{(i)}\}_{i=1}^K$
-

H. Additional text generation result

We display results on text generation control when using the DEFT guidance term. We find that:

For toxicity-controlled generation, SMC-based methods outperform guidance on control metrics across the guidance temperature range $[0.0, 2.0]$, which is even more apparent for higher SMC temperature α . This is at the expense of a slightly degraded perplexity compared to guidance. At high guidance temperature, the guidance method is on par with SMC-based methods on toxicity score, at the expense of a significantly deteriorated perplexity. This indicates that at high guidance temperatures, the samples deviate from the fine-tuned data distribution. In that scenario, a good balance between perplexity and control generation is in the mid-to-low range of guidance temperature.

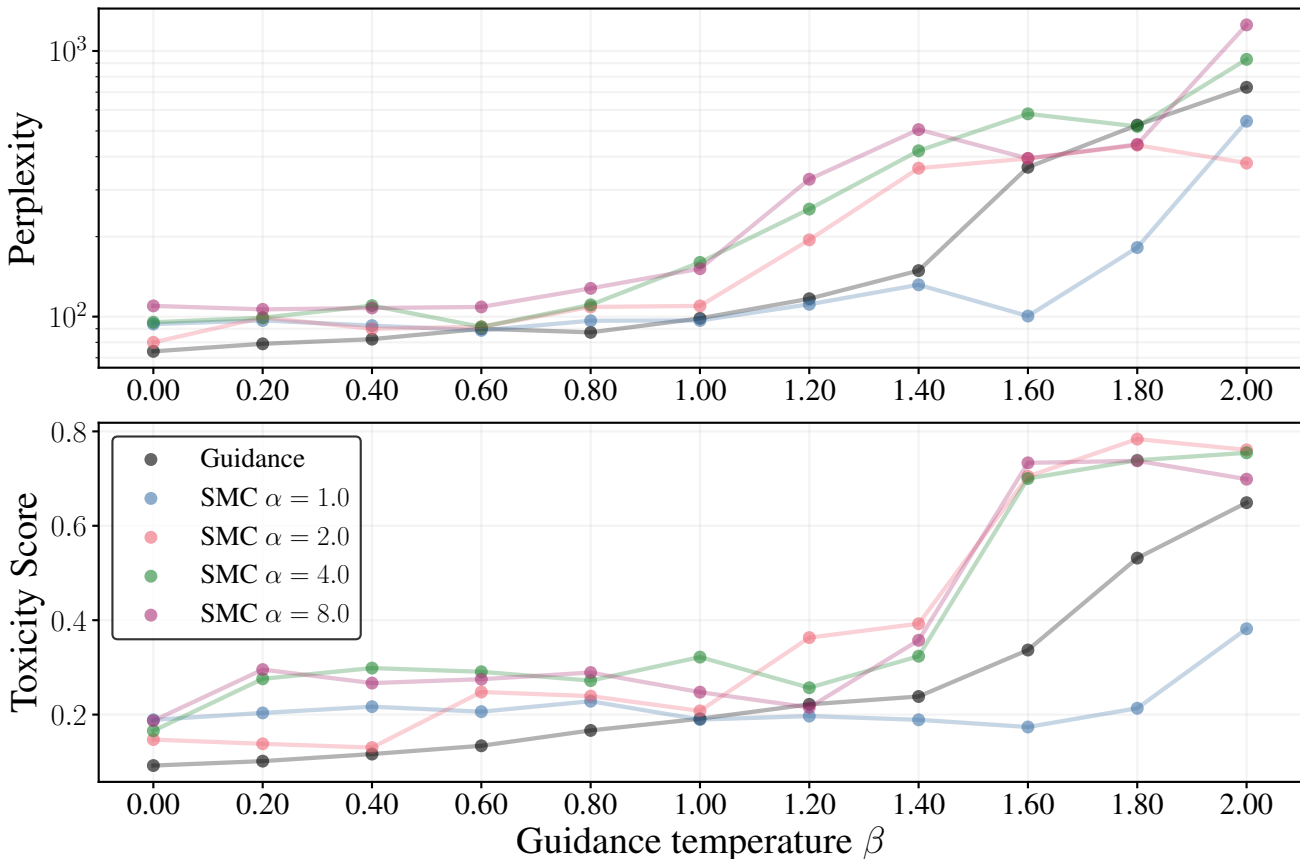


Figure 8. **Toxicity controlled generation:** Guidance is performed with DEFT. SMC methods show improved toxicity scores across all proposal temperatures β , particularly for high β , demonstrating enhanced generation control.

For text infilling, SMC-based methods achieve superior accuracy for guidance temperatures $\beta \in [0.2, 0.8]$. However, at high guidance temperatures, both SMC and guidance methods attain comparable optimal accuracy and perplexity. In this specific scenario, despite lacking theoretical guarantees, the guidance method proves more practical due to its lower computational cost while maintaining equivalent performance.

For sentiment-controlled generation, SMC methods achieve higher accuracy for guidance temperatures $\beta < 0.6$, which comes at the cost of a slight increase in perplexity. At higher guidance temperatures ($\beta > 1.2$), both SMC and standard guidance converge to similar accuracy levels around 0.85, with comparable perplexity until $\beta = 1.6$. Beyond this point, all methods show significant perplexity deterioration, with SMC methods exhibiting slightly higher perplexity than standard guidance.

Debiasing Guidance for Discrete Diffusion with Sequential Monte Carlo

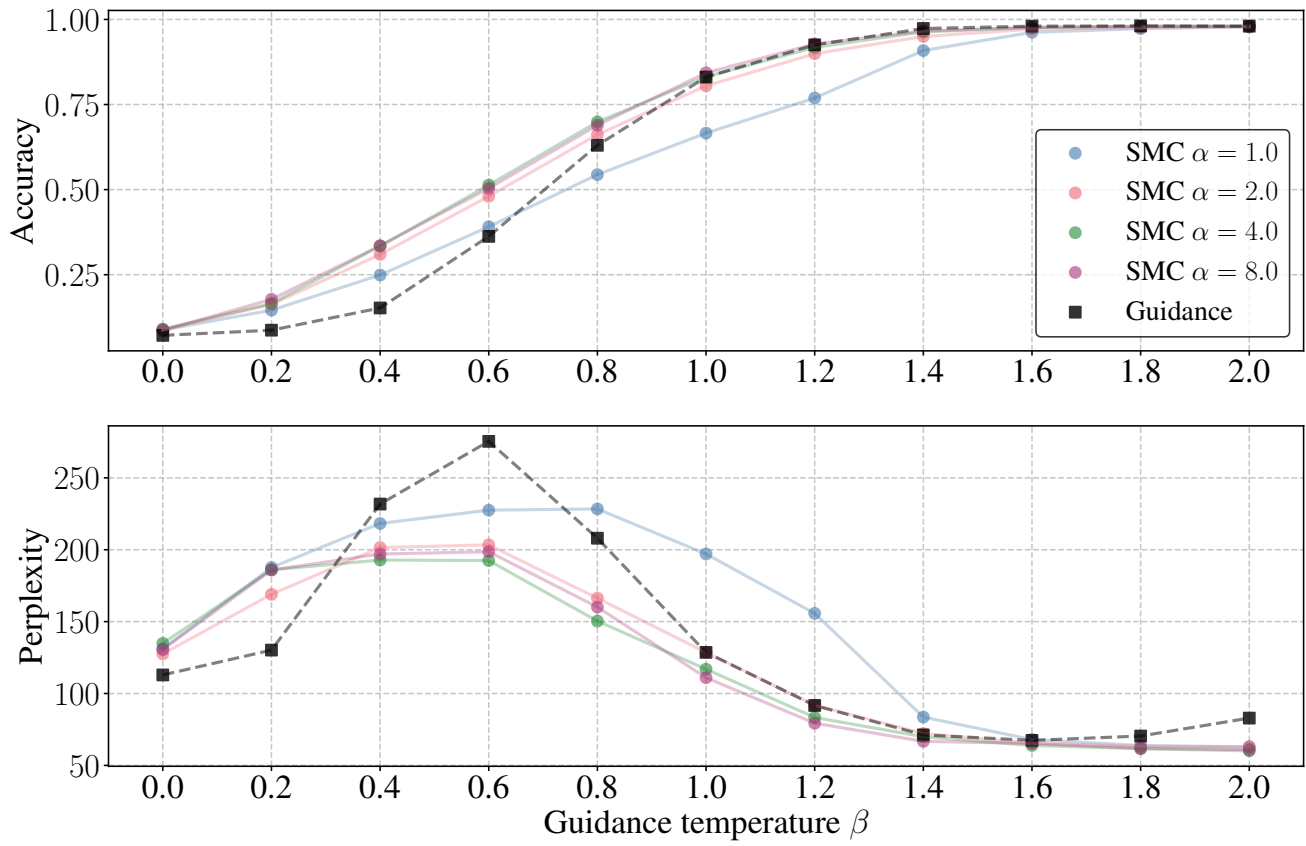


Figure 9. **Text infilling:** Guidance is performed with DEFT. SMC based methods show improved accuracy for $\beta \in \{0.2, 0.4, 0.6, 0.8\}$ while keeping a lower perplexity for $\beta \in \{0.4, 0.6\}$

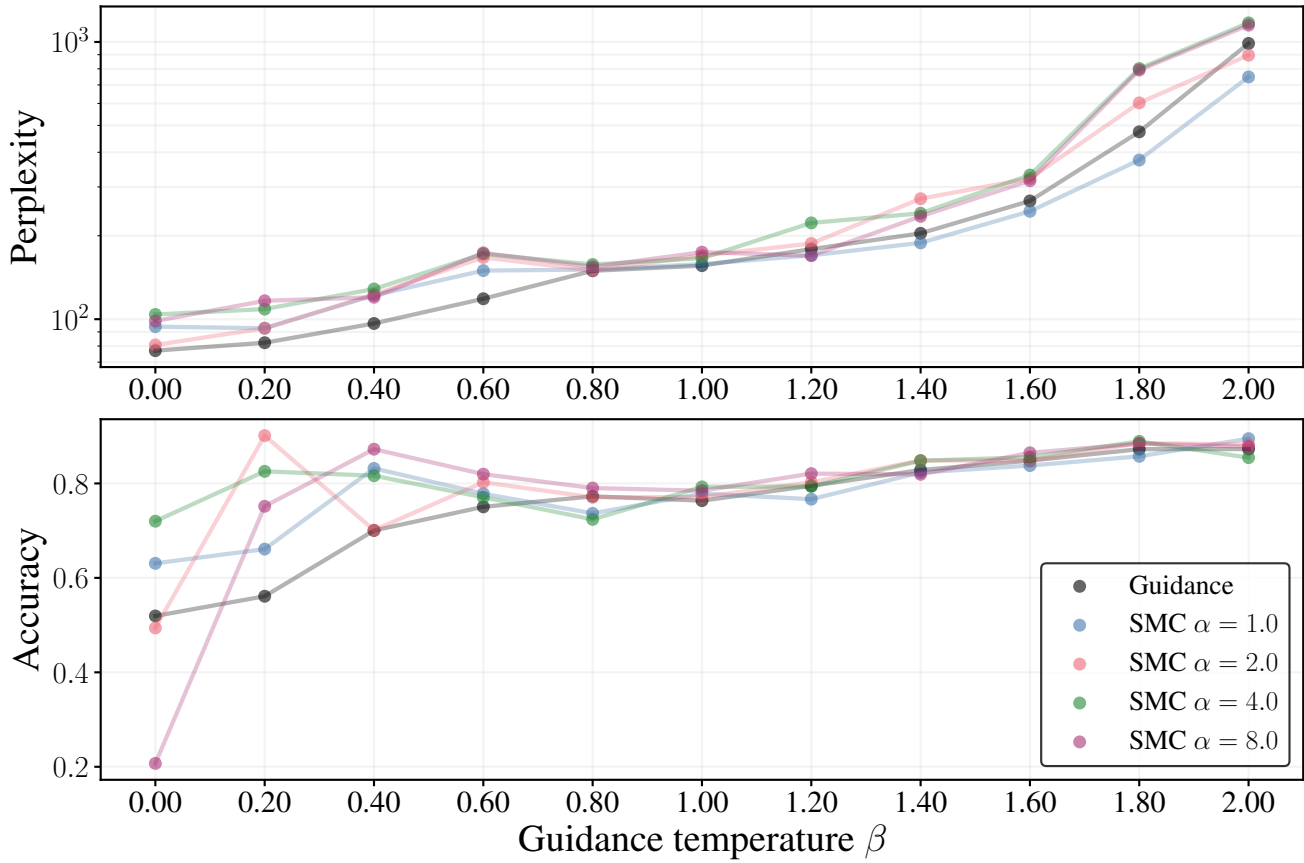


Figure 10. **Sentiment controlled generation:** Guidance is performed with DEFT. For guidance temperature lower than 0.6 SMC methods show improved accuracy while having higher perplexity. For larger guidance temperature accuracy and perplexity are relatively similar.

I. Samples

ant EOT a very funny and rewarding small comedy . EOT a rather else altogether EOT genuinely sweet and EOT evokes its low-budget constraints fairly well EOT , evocative EOT 's spooky . EOT an interesting concept EOT here 's the treat . EOT a solidly entertaining film in its own right EOT supremely goofy pleasure EOT demonstrated extraordinary faith EOT an unflinching meditation on how business can change those who enter EOT love the film . EOT – deep down you 've a family EOT a fascinating glimpse EOT of place with its oscar-worthy predecessors EOT pounding, offering fine acting moments , EOT it 's a surest bet EOT an engaging fantasy EOT , the material actually springs to life EOT director credit gyllen brings together caine and grant EOT star charisma EOT consistent EOT what 's best about dustin gondry 's sophisticated read my lips EOT EOT ... scotches . EOT 's surprisingly faithful EOT EOT dazzling EOT make up for the execution 's weak comic buttons . EOT curiously funny, intriguing , EOT just that satisfying exploration of love and companionship EOT EOT emotional sympathy EOT make it entertaining , EOT ungainly work EOT strongest films EOT funny EOT to sharp writing EOT make for a great director 's to make, everlasting EOT innocence EOT though not technically proficient or as EOT remark to ' believer ' in some time EOT sometimes insightful writer EOT mr. honorably EOT and unforgettable characters EOT cool, cocky, and – dare i say twice – hollywood-esque EOT powerful story EOT surprisingly sweet EOT engaging, compelling tale EOT beautiful EOT vibrant air EOT but ultimately winning film EOT its simple expressiveness EOT enriched than limited by its exceptional lead performances EOT of impressively challenging social drama EOT the rich formalism EOT EOT keep you EOT of laughs EOT quieter EOT the praises EOT some monster movie EOT as his penchant for documentaries EOT is latin star to young international hip-hop audiences EOT often funny romantic comedy EOT smoother EOT only enhance his good looks EOT immensely enjoyable EOT one of the most idiosyncratic comedies EOT oddly watchable EOT ambitious EOT directed personalities EOT interesting, i must say , EOT faithful , EOT well, EOT well lived EOT compelling and gripping EOT everyone 's comic relief EOT truly funny EOT enjoy EOT elegant delivery EOT idea EOT familiarity EOT to hold you well past its 90 minutes EOT find love EOT fresh sense EOT has spliced together bits and pieces of hagney 's reign EOT for good, scary movies EOT gaining this movie EOT flaccid satire , EOT EOT respectable, sweetly adventurous EOT a film EOT smart and subtle EOT vibrant and EOT their fathers EOT her maternal fury of faith EOT EOT protagonists EOT is surprisingly insightful and fun and entertaining EOT that acts as if it never had any idea what EOT , originality and technical skill EOT argue EOT above all, blue crush is nothing to overlook . EOT sulky and beautiful rendering of an intense mystery about the world 's greatest teacher EOT daring teacher EOT cinematic stamp EOT warm , EOT its inviting EOT sexy EOT is realistically terrifying EOT a surprising entree EOT invigoratingly irresistible EOT action-power appeal EOT slyly debated film EOT mention, engaging premise EOT , there are enough laughs to keep on clicking through EOT puts us off-center in the unfolding of bielinsky 's clever scenario , EOT the local flavor and french musicmaking traditions EOT elegance EOT it has a real “ story ” EOT at least the funniest idea EOT works well on different levels, until it is actually funny . EOT , cleverly crafted and EOT scenes brimmed EOT allows you to forgive its basic humanity EOT that tickles the chills of EOT subtle EOT the film a stunning lesson in human-scale acting , EOT 's a film school exercise with dignity and wit that “ should have been right to grow up EOT a riot like john ritter 's brothers ... EOT thumbs up EOT seemingly EOT they 're the target audience because EOT sensitive performances and EOT magnificent landscape EOT caric ballot EOT bring more goodies . EOT as cohesive , EOT some first-time director EOT of the finest kind EOT a spirited EOT 're out tonight EOT style and color EOT a cleverly written and thoroughly winning portrayal of titular kid a woodman who 's become a self image with kids EOT emotional evolution EOT she 's a tempting bouquet – if you live a minute ... come and see the charm of the movie EOT is credible EOT a classical actress EOT delicious camera work EOT a treat , EOT a more absorbing piece EOT all builds up to the easy, endearing knockout . EOT still charming – likely his next film wo n't be the greatest date movie EOT , sweet EOT . EOT most good-hearted EOT a few good ideas EOT a feel-good thriller EOT , illuminating study EOT large metaphor EOT successful EOT fresh is “ fresh ” again EOT tell this tale EOT felt and affecting EOT

Figure 11. Sentiment control - positive samples - SMC $\beta = 1.0$, $\alpha = 2.0$. EOT indicates End Of Text

having a difficult time telling what time in the past year . EOT a pale successor EOT an odd bit of an erratic EOT killing time EOT wobbly EOT mean-spirited EOT 's no energy EOT carries little insight on either end of the other EOT dangerous comedy EOT a slightly flat , EOT the little the seams EOT EOT it drags EOT perverse EOT this bland EOT the cheapness EOT poorly EOT any teen movie starring slackers or EOT succeeded EOT brain strain EOT ill writing EOT may also not have been the grossest american bike movie of 2002 . EOT absurdities EOT it 's too simpleminded – EOT has the idea been sealed in a jar EOT this obvious rip-off EOT racist EOT is wit, or even good acting , EOT more like satire than illuminating examination EOT despite snow dogs, leaves us cold . EOT the action is predictable with many subplots and EOT very insecure EOT 's still flibbled together its clichés . EOT bad combination EOT particularly suspenseful at times EOT deep technical blues vs blues EOT are so smeary, blurry and jagged EOT form 51 is n't really scary enough for “ midnight flick ”, and EOT thought you or i were paying full price for this, and rent those instead EOT is a minor miracle EOT handbags in saving private ryan EOT like ‘ to suck ’ EOT its clichéd scenes of war EOT poorly dubbed dialogue, and EOT 's hard to imagine a product more repellent than adam sandler 's 2002 EOT EOT weighted a sci-fi story that 's bottom-heavy and tired EOT wrong things EOT stiflingly EOT EOT endless exposition EOT simply overcooked EOT evasive EOT call an “ ambitious failure EOT EOT even less ambitious failure EOT ridiculous and sloppy EOT no air conditioning EOT the ragged pacing EOT a loud, crassly predictable rehash EOT how lame it all is EOT ends world traveler 's lackluster title EOT have done with all the subtlety from earlier had taken in favor of more user-friendly computer tutorial EOT EOT mind settles into a irksome parade of human frailty and death . EOT smug and exploitative EOT the whining EOT this latest comedy tangents of pratfalls, injuries and pranks EOT to anyone who suffered through halfway through david rifkin 's sweet home ‘ alabama EOT old pickup EOT should have been ordered off the screen EOT like the plague EOT neges toward fuzziness EOT its skewed acting , EOT an odd, painful and obnoxious attempt at a documentary EOT , repetitious and contrived EOT lacks a moment of considerable poignancy . EOT chaos and EOT EOT cold, emotionally opaque EOT stands nowhere EOT frustrating EOT dull EOT suffered EOT characteristic quirks EOT half-step EOT , it 's hopeless . EOT there 's nothing new to be taken from ‘ fatal attraction ’ 4ever EOT is painfully bad . EOT unfaithful hollywood fluff EOT have little interest in jez begley 's book EOT no foundation for disney EOT EOT , herzog is the director 's logistically and EOT is it not hagiographic, though EOT need more than plot EOT rocks and holes EOT with lots of solips EOT ving EOT at times maddeningly repetitive . EOT rendered all round square edges, blurry images and murky and EOT 's cloying, manipulative EOT trial EOT on sub-zero animation EOT an annoying , EOT went to the restroom but want my money back . EOT water torture EOT pompous EOT rigid idea EOT insufferable EOT as boring and pedestrian EOT , heavy-handed EOT marginal insights EOT from lost ring to snatch on stage EOT hampered by a shabby script EOT gold is a real hollywood dog story EOT limpid and pretentious endeavor EOT is subtler than it might have been . EOT the film with relentlessly nasty situations EOT 's not handled well EOT wastes dialogue EOT sensible violence EOT of all the male junkie post-about obsessive relationships EOT is a testament to the author 's work EOT have had room for more creative action . EOT empty farce EOT liar zone EOT could call it tacky EOT painfully awful EOT forget about the fact that kennedy has nothing to offer up his act EOT the faintest hopefulness , EOT EOT flat EOT , spiteful idiots EOT is superficial and EOT describe characters ' frustrations EOT end zone EOT familiar and thoroughly recycled plot . EOT tired EOT aimless direction, pathetic acting, heavy dialogue, tissue-thin characters EOT EOT of inept filmmaking EOT last 15 years EOT the picture just EOT nothing except they ca n't – anything, really, seems to matter very much EOT a noticeable amount of its own EOT neat EOT best elsewhere EOT waste ; EOT human behavior , EOT too fancy EOT derivancy EOT distinct comic direction EOT this m-out-l lesbian comedy EOT does n't give a complete picture . EOT shallow plot EOT could have any interest in silly fluff EOT , tedious , EOT 's not clear what this turkey is

Figure 12. Sentiment control - negative samples - SMC $\beta = 1.0$, $\alpha = 2.0$. EOT indicates End Of Text

or it really costs that far to finish rail. EOT I always thought the part time NDP would be on the hook for this, but then they had to master the ndp's fiscal policies. EOT Fess up..... EOT He managed it brilliantly. EOT You are wrong in that regard. Harper suggested enough to leave the potential harm to children (and adults) to see. EOT Agreed. Further increasing the income of Quebec will likely lead to increased income tax charges for Ontario governments attempts to do same. EOT rumps.. the globe loses again.. its only readership is NK EOT once again putting alt lunatic whining over the real picture bud EOT Alaska hasn't cut the PF yet Walker over spent our PFD for the same 40 years. Walker has 3 more session to do some cuts cutting back PFD dividends not PFD raiding the new gas line. Enough Permanent fund cut already Walker and Governor Walker and Governor Walker. Time for legislature and real leadership in Alaska needing new taxes. EOT Yes Bravo Orange Pail! EOT Sorry son but don't look forward to Ducks game, it's always good to find out who has the better quarterback. EOT Trump is fleeing the Trump administration right now. EOT Sorry, you've undermined the whole point of your comment ... EOT How about everyone familiar with Dale Wright? EOT One less Hawaii Democrat. EOT Where's Cory Gardner. EOT Silly Senate. EOT Happy New Air Canada - what a touch of sweet irony. EOT Great comments! EOT Seems like your actions out in front of the world for all people to see. EOT there is no illegal world building EOT Trudeau ? EOT Not to fast.....tax Vancouver got it fair share. EOT LOL..... EOT Maybe our Senators Cory and Murkowski will vote for a repeal. EOT This is about criminal charges underway and emails continue to be the target. Mueller will investigate the names Hillary, let Mueller have his look and hopefully does find Hillary exists. EOT I'm sure snakes are the least human kind. EOT Great pleasant surprise. EOT I agree with you! EOT The problem is that guys like Meredith and Crapwell will just fade away. EOT Alceste three times is running as a republican. EOT Wrong case. Can't find a place right there. EOT <http://JustPeace.org> That's Fairbanks, Fairbanks EOT Yep. His opening rhinos ring louder every posting. EOT Not China nor NK. Neither have threatened NK. EOT Maybe they break the law along with other citizens who drive motorized vehicles. EOT What were you wearing? Wear the ladies locker? EOT Get a clue who play each string on the violin. EOT I have been discouraged about owning a home when rental prices have gone down significantly. It seems like there is only reason for gray market rentals any more. If I could find an area that had a small amount of rental units and never close it with no decision but rent, then I could buy in. EOT More Liberal tabloidism fleeced by paid leftist disinformation efforts. Good riddance! EOT Didn't happen to read your post either. EOT Wrong Old Spice.... EOT IRT Gary Crum, we don't need any new information when it comes to responding to the DP. EOT why? EOT Then why tax the PFD earnings when Anchorage borough and developers pay local property taxes with PFD earnings? EOT Agreed! Pay you to Netflix any network programming than you get in actual services you pay for. EOT You wanted Hillary is a lot different than wishing Hillary lost..... EOT Does every car require a plate handle or do democrats have ? EOT They have not given up anything re producing soft fishing. The dairy industry will not be on any side of the deal when NAFTA gets a bad looks up. First side to lose the deal is at risk. EOT Agreed. EOT I assume it isn't you Gary EOT Yeahhhh trump juice! EOT I remember long ago the Cons and the NDP were slamming each other behind the scenes. EOT Your tolerance must be getting really old. EOT Wouldn't say Amy hasn't heard here. EOT So Berkie and Caldwell belong in jail? EOT the big question is "which will they write it" EOT How was this deficit announced 6 months ago? EOT Very good article thanks for posting Vic. EOT Completely untrue. South America is producing the most efficient portion of the world's oil soon. BTW, if your planning on expanding pipelines, move ahead and avoid Alberta. EOT Wow. Can't even conceive of imagining how naive trumpsters are. EOT Nah. It was a big one. EOT Prove it. Tax my dividend too. EOT Did't the letter writer say Lame County? EOT Yep! That's who you "democratic" voted into office. EOT EOT Agreed! Harper! Has to go. EOT Sorry but not quite. The data you are referencing is one game show. EOT So Alaska needs our own modern rail system? We don't need a modern system of satellites like the majority of lights on the nation. EOT I find it hilarious that idiot trump does nothing to mitigate

Figure 13. Toxicity control - non toxic samples - SMC $\beta = 1.2$, $\alpha = 4.0$. EOT indicates End Of Text

when commuters were most busy..... EOT Eh. Used that logic. EOT Better hope the coming recession never happens EOT Enough with your infomeration Bombing homes works better. EOT Just keep Trump in. It could be our destiny to get rid of all Obama's puppet masters EOT Here's my only thought regarding your comment: Keep up! EOT How did I need any further contribution to that? EOT Someone please refute my fact. EOT The phony Liberals who "thought" a love of country above party will have no spine. As always, the press will focus on facts and Republicans will relentlessly call out real Liberalism. EOT That's a fact. Comey's firing does have been the direct result of Comey's conduct acting inappropriately for US intelligence. Comey is not the person fired out of political motivation, but Trump was rejected as for the US Criminal Code but rather the federal judge has rejected him. EOT ": An extension for the appeal period or even an extension for each waiver signed may be all Kobachak's congressional breaks." As I pointed out in a Civil Comments form on behalf of Kobachak in 2016 there was nothing further to see in Kobachak's case. He picked a fight and all is well with his formerly a non-friend and ally. EOT So? The author is anonymous? at least he doesn't have a secret. BTW, you seem to assume that Kobachak doesn't share your own psychology. Darn it. EOT I am a retired member of the Sierra Club, although I am also a member of the California chapter at <https://fight.org/> and the Northeast chapter at <https://www.sanfrust.org/> The health issue in Puerto Rico is significant and I think about it from a personal perspective. Trump is really sparking passions in his comments so will face criticism. Aside from that aways, he needs to understand what actually took place in Texas City and events that resulted in this disaster there. EOT Our government is only better than you. EOT Now that Trudeau has been given free rein in unilateral withdrawal from the U.S., then why would we subject ourselves to further a significant trade relationship that the Chinese and Russians absolutely want? It can only work here if we remove big historical barriers such as the Suzuki's and tackle these for our benefit. The world is entering a new era of mutual respect. EOT This is more of exactly what's expected. EOT That's wording that selectively is used. Only a few extreme views dominate the discussion. These are only three of 10. EOT More that some people do disagree with the process as they may have alternative theories. I also suggest you get educated and understand the current science and the reality of climate change. EOT Aloha, go year long in different neighborhoods like season after year. I see day in and day out the exact same homeless; no different penalty for visiting Eugene; same as anywhere else. EOT Thanks for the linking C of B page to Quebec. Donna can't cut it. EOT The crime is not unusual, per say. They are allowed their privacy, but selectively. No tunnels to break, but it is a crime. EOT The IPCC failing to release public information regarding the case runs contrary to the article's recommendation. Quite clearly his fate is not to be ended in death as was indicated by the way he was raised when confronted with simply not being born. EOT Again, are you not proud of your experience and reach? EOT I agree. This analysis does not take into account that the content of most of our English-language newspapers is particularly bias. To what appears to be happening in Canada a few days, but every once in a while a Canadian newspaper is going to highlight certain facts because of the importance a story that few would know. It has also been said that many newspapers insist on showing all news every week and not just the stories that are the most important. EOT If i can looked at things differently and see more from the top - it emerges I see less as 'completely out of line' as others feel I have looked more towards the 'top'. EOT We are all doing the best we do, sometimes it takes the next thing. EOT Having a minimum wage for the smaller employees in Alaska must be expensive because the businesses have to do their work at home thru government, education and the overall economy. My monthly cost of organic food is \$10.71 per hour plus. So how can I go through the trouble and earn that many per hour rather than having a loss on these goods? I paid lucky so I will have to stock up while in retirement, but that is still very expensive. Remember you not only need the help with government but with income, earned through education, and the rest of the economy. EOT Sure, a lot of kids are taking hitches and missing their focus. The selection of character, athleticism and tougher focus is what determines the chance of success. EOT It's not everything. He did hate the west in his first election. EOT It's the First Amendment folks to blame ... I say to "vide wolf, flock"

Figure 14. Toxicity control - non toxic samples - Guidance $\beta = 1.2$. EOT indicates End Of Text